8411-6001-RU000

STUDY OF LUNAR LANDING
SENSOR PERFORMANCE
INTERIM REPORT NO. 2

NAS 8-5205

31 OCTOBER 1963

PREPARED FOR

GEORGE C. MARSHALL SPACE FLIGHT CENTER
HUNTSVILLE, ALABAMA

TRW SPACE TECHNOLOGY LABORATORIES
THOMPSON RAMO WOOLDRIDGE, INC.
ONE SPACE PARK • REDONDO BEACH, CALIFORNIA

8411-6001-RU000

STUDY OF LUNAR LANDING
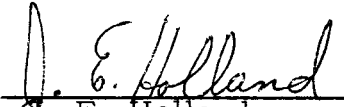SENSOR PERFORMANCE
INTERIM REPORT NO. 2

NAS8-5205   31 October 1963

Prepared for

George C. Marshall Space Flight Center
Huntsville, Alabama

Prepared by _J. E. Holland_
J. E. Holland
Project Engineer

Approved _J. Heilfron_
J. Heilfron
Director
Guidance Laboratory

TRW Space Technology Laboratories
Thompson Ramo Wooldridge, Inc.
One Space Park · Redondo Beach, California

CONTENTS

ILLUSTRATIONS

ILLUSTRATIONS (Cont'd)

1. INTRODUCTION

Interim Report No. 2 for the "Study of Lunar Landing Sensor Performance" has been prepared by TRW Space Technology Laboratories (STL) for the George C. Marshall Space Flight Center (MSFC) under Contract NAS 8-5205. This report represents the completion of the tasks delineated by Modification No. 1 to the subject contracts.

The first phase of this study was directed toward the following goals:

o   Determining sensor requirements for effecting soft lunar landings from direct approaches and orbital descents,

o   Modifying STELATRAC as required to achieve the requisite sensor capability

o   Delivering a solid-state power source capable of providing more than 100 mw at 10,347 mc when driven at 646.7 mc with an input power of 2 watts.

The initial requirements study was predicated on the use of a solid-propellant vehicle on a direct radial approach and a liquid-fueled vehicle employing low-altitude staging for orbital descents. Near the terminus of the above effort, it was requested that the Multimission Module be investigated to ascertain its effect, if any, upon sensor requirements. Towards this objective, MSFC supplied STL with representative descent profiles of a Multimission Module on a powered, orbital descent and on a minimum-fuel Hohmann transfer, both originating from a 220-km, circular, lunar orbit, for utilization in deriving estimates of the sensor parameters. Concurrently with this derivation, the sensor characteristics for effecting a soft landing of a Multimission Module on a direct radial approach to the lunar surface were generated by STL using hand computations in conjunction with several simplifying assumptions.

Under modification No. 1 to the subject contract, STL was authorized to perform a more complete assessment of the sensor characteristics for

effecting a soft lunar landing via a Multimission Module and to investigate any required STELATRAC modifications to assure compatibility with the requirements. These two tasks constitute one portion of Modification No. 1 to the subject contract. To fulfill these tasks, a two-dimensional trajectory study was conducted to determine the sensor parameters necessary for consummating direct and orbital lunar descents via the Multimission Module. A two-dimensional study does not permit the determination of out-of-plane angles or slant range to an implanted offset beacon. However, sufficient estimates for defining performance envelopes can be made from an examination of the pertinent geometry near touchdown.

The third task of Contract Modification No. 1 emanated from the design effort devoted to an Extended Range Altimeter during the initial phase of the subject contract. At that time, a high-precision and low-threshold sensitivity gating and error-sensing technique was studied analytically in appreciable detail. However, the analysis was restricted in scope because of the nonlinear character of the attitude tracker; i.e., as the altitude decreases, the loop gain and bandwidth should increase. To fully assess the performance potential of the altitude tracker over typical descent profiles, either a simulation study or an experimental investigation was indicated. (The former was chosen as being more expedient and economical in this instance.) In addition to confirming the accuracy potential, it was necessary to establish the effect of vehicle maneuvers and determine the altitude interval over which no loop-bandwidth change would be required. A hybrid simulation was configured using both digital and analog equipment, and representative Multimission Module descent profiles were "flown" while the altitude tracker performance was appraised. A hybrid simulation was employed to achieve the simulation flexibility and accuracy possible with digital equipment while retaining the ease of parameter adjustment associated with an analog facility. An on-line arrangement was planned wherein the data was directly plotted for analysis during the computer run. As a result, a rapid and efficient simulation study could be effected.

2. SUMMARY

The first task to be performed under Contract Modification No. 1 consisted of the determination of sensor performance parameters for soft-landing a Multimission Module on the lunar surface. The spacecraft was to be on either a direct approach or an orbital descent from a 200-km, circular orbit. In fulfillment of this item, two-dimensional computer programs were prepared for the two classes of descent, including an offset landing when beacon-assisted. The offset orbital descent consisted of an overfly to a landing area 9.3 km from the beacon and in the descent plane. The pertinent parameters used to establish the descent profiles are tabulated in Table 2-1.

Table 2-1. Vehicle Parameters Used to Determine Profiles

	Orbital Descent	Direct Approach
Initial earth weight before burn	67,500 lb	79,400 lb
Thrust	30,000 lb	30,000 lb
I_{sp}	440	440
Trajectory	Hohmann transfer from 148 to 15 km	72-hr flight time on radial path
Start of burn	Altitude of 15 km	Altitude of 744 km at 584 sec before time of final position
Final position	Altitude of 305 meters with velocity of 0.03 m/sec and acceleration of 5 m/sec^2	Altitude of 305 meters with velocity of 9.1 m/sec and acceleration of 5.9 m/sec^2
Pitch maneuvers	Constant pitch rate of 0.12 deg/sec after start of burn until 2 sec from final position at which time an instantaneous* pitch of 63.5 deg is executed	none

* An instantaneous maneuver was used in the study; however, in practice this would be performed slowly as part of a hovering maneuver.

With the descent profiles defined, the parameters of range, slant range, and altitude and their respective first and second time derivatives and the angle and angle rates and accelerations were determined for the Multimission Module on the reference descent profile. In most instances, the requirements were within the envelopes established in Interim Report No. 1 for this contract.[*] The significant differences are an increase in the range/altitude capability to 800 from 700 km and larger antenna-pitch-axis gimbal freedom for both the beacon tracker and Slant Ranger Tracker-Velocity Meter. The Multimission Module sensor requirements are presented in Tables 2-2 and 2-3 for the beacon-assisted and non-beacon-assisted descents. The sensors for the non-beacon-assisted descent consist of an Extended Range Altimeter for determining the thrust profile while accomplishing main braking, as well as measuring altitude while in lunar orbit; and a Slant Ranger Tracker-Velocity Meter for terminal guidance purposes. The Extended Range Altimeter is integral with the beacon tracker.

Interim Report No. 1 discussed the necessary STELATRAC modifications to configure it for tracking a lunar beacon. The additional considerations evolving from the Multimission Module study pertaining to a beacon-assisted landing are an increase in range capability to 800 km and gimbal freedom in the pitch axis of 120 to 150 deg.

The former can be accommodated without any changes in the beacon tracker described in Interim Report No. 1 (see, for example, Figure 2-1 therein). The second necessitates a slightly heavier (3 lb) antenna assembly. The additional weight arises because of a probable increase in the lever arm attached to the pitch axis to achieve the increased angular coverage which results in a heavier assembly. If the vehicle pitch coordinate were pro-grammed differently than the reference trajectory near touchdown for the overfly case, i.e., a pitch rotation rate of 6 deg/sec or less in lieu of an instantaneous rotation of 63.5 deg, the gimbal freedom requirement can be reduced to 120 deg. Lastly, since a minimum acceptable elevation angle of 10 deg precludes obtaining accurate data for ranges in excess of 50 km, a steeper trajectory is indicated which again will alleviate the angular coverage requirement in the pitch plane.

[*] "Study of Lunar Landing Sensor Performance," Interim Report No. 1, NAS8-5205, 21 June 1963, by TRW Space Technology Laboratories (formerly Space Technology Laboratories, Inc.)

Table 2-2. Sensor Requirements for Beacon-Assisted Descents

Quantity	Measurement Interval	Accuracy (3σ)
Range	0 to 800 km	0.05%[*] ± 1 m
Range rate	+300 to -2500 m/sec	0.15 m/sec
Range acceleration	-8 to +27 m/sec^{2}[**]	---
Angular coverage	Pitch plane 120 to 150 deg;[***] Yaw plane 60 deg	0.3 deg
Inertial Angular rate	8 deg/sec	0.03 deg/sec
Inertial angular acceleration	0.6 deg/sec^{2}	---
Vehicle angle rate	6 deg/sec	---
Vehicle angle acceleration	3 deg/sec^{2}	---
Beacon antenna coverage	2 lobes near horizon, diametrically opposed; 1 lobe vertical	---

---

[*] An accuracy of 0.05 percent is required for orbit determination while in lunar orbit. Otherwise, accuracy specification can be relaxed to 0.5 percent ±1.0 m.

[**] 27 m/sec^{2} is only required for a high F/W spacecraft.

[***] Depends on final pitch profile near touchdown.

Table 2-3. Sensor Requirements for Non-Beacon-Assisted Descents

Extended Range Altimeter

Quantity	Measurement Interval	Accuracy (3σ)
Altitude	1. 8 to 220 or 800 km[*]	0. 5%
Altitude rate	0 to -2500 m/sec	**
Altitude acceleration	0 to 9 m/sec^{2}***	---
Antenna coverage	60 x 60 deg	---

Slant Range Tracker-Velocity Meter

Quantity	Measurement Interval	Accuracy (3σ)
Slant range	0 to 10 km	1% ± 1 m[****]
Slant range rate	0 to -550 m/sec	1% ± 0. 5 m/sec
Slant range acceleration	0 to 9 m/sec^{2}	---
Lateral rate	0 to 120 m/sec	2% ± 0. 5 m/sec
Angle from vertical	0 to 70 deg	---

[*] Necessary for initiation of main braking on a radial descent trajectory.

** Difference attitude rate if required.

*** This value of acceleration is based on a F/W = 1 spacecraft capability, wherein the thrust is directed vertically. A higher acceleration magnitude will not unlock the altitude tracking loop of the receiver, but will increase dynamic errors.

**** Bias accuracy of 1 meter holds near vertical incidence.

For the non-beacon-assisted descent, a problem originates from the vehicle attitude being nearly horizontal during a large portion of the terminal phase so that the axis of the SRT-VM antenna assembly intercepts the lunar surface at an angle of about 20 deg from the horizontal. There is no feasible alternate other than gimbaling the antenna assembly in the pitch plane. A torque motor drive assembly is recommended to move the antenna between two limits. One limit directs the antenna assembly axis along the vehicle longitudinal axis, while the other rotates the assembly 40 deg from the vehicle axis. The weight increase because of the drive assembly is 4 lb. The power required to drive the motor is negligible since the motor would be operated a maximum of once during a descent.

The sensor characteristics shown in Interim Report No. 1, Tables 2-3 and 2-4, are modified in the areas depicted in Table 2-4 below.

Table 2-4. Modified Sensor Characteristics

Beacon Tracker	
Antenna freedom	
Pitch	120 to 150 deg
Yaw	60 deg
Range interval	0 to 800 km
Weight	
Radar antenna	26 lb
Slant Range Tracker-Velocity Meter	
Antenna gimbal freedom	0 and 40 deg in one discrete step
Antenna weight	8 lb
Mean-time-between-failure OGO type parts	149,000 hr

Concurrently with the trajectory study, a simulation of the Extended-Range Altimeter altitude tracking loop was performed. A hybrid facility was used to improve the simulation accuracy, provide an on-line capability and expedite trajectory profile data read-in. The descent profiles employed were those generated during the trajectory study supplemented by a test case to provide a means for comparing the dynamic response with the analysis of Interim Report No. 1. The initial choice of tracking-loop parameters was made using the analysis in Interim Report No. 1 and variations

about the parameters were then examined during the study. The performance
of the tracking loop under varying dynamical situations is summarized in
Table 2-5.

Table 2-5. Typical Altimeter Tracking Errors[*] From
Simulation Program (Multimission Module
Trajectories)

Effective Tracker Bandwidth[**]	Dynamic Lag Error (percent)	Thermal Noise Error (1σ)[***] (percent)
ORBITAL DESCENT		
Case 1	< 0.50	< 0.50
Case 2	< 0.10	< 0.90
Case 3	< 0.05	< 1.60
VERTICAL DESCENT		
Case 2	< 0.30	< 1.22
Case 3	< 0.05	< 1.70

The dynamic lag errors occuring for small B_N can be removed from
the data by appropriate processing in conjunction with information relative
to vehicle dynamics. Additional smoothing of the noise error external to
the analog circuitry will, of course, reduce it. Dynamic errors are largest
during the terminal phase, while noise errors are significant at maximum
range. Maxima in both error categories do not occur simultaneously.
In conclusion, it is confirmed that the performance of the altitude tracker
is commensurate with an error tolerance of 0.5 percent (3σ) for the typical
descent trajectories.

---

[*] These errors can be reduced by further smoothing external to the
altimeter if required.

[**] Effective tracker bandwidths (B_N) switched approximately at decades
of altitude, loop gain adjusted continuously; Case 1: B_N (cps) = 0.1,
0.3, 1.0; Case 2: B_N = 0.3, 1.0, 3.0; Case 3: B_N = 1.0, 3.0, 10.0

[***] The errors listed occur at maximum altitude and decrease as $\sqrt{h}$.

3. MULTIMISSION MODULE SENSOR PERFORMANCE REQUIREMENTS

A trajectory study was made to determine the requisite sensor requirements for effecting a soft lunar landing via a Multimission Module on either an orbital descent or a direct-approach trajectory. To expedite the study, it was decided to limit the scope of the computer trajectory programs to two dimensions. At long ranges, the two-dimensional approximation is valid for the establishment of parameter envelopes. At shorter ranges, the computer results can be supplemented by an investigation of the touchdown geometry for the case of an offset landing from an implanted beacon. Trajectory data were obtained from digital computer programs for two different descent profiles: one an orbital descent and the other a direct radial approach. These profiles represent the extrema of possible descents and hence have merit in establishing sensor envelopes. Additional computer studies were made for beacon-assisted descents to a landing site 9.3 km downrange from the emplaced beacon on the lunar surface. Data from the computer trajectory runs were evaluated to ascertain whether the envelope of sensor performance parameters as stated in Int. Rept 1 for both the beacon-assisted and non-beacon-assisted descents were sufficient to encompass the requirements of the Multimission Module and, if the envelopes were not inclusive, to determine the changes needed. Some study time was directed toward examining sensor requirements for other mission phases.

3.1 Multimission Module on Direct Approach

The pertinent data employed to specify the trajectory for the direct radial approach are presented in Table 3-1. Two different cases were considered: the first case was a landing on an emplaced beacon and the second a landing 9.3 km from an emplaced beacon.

For the direct-approach landing with no beacon offset, the range[*] R,
slant range[*] R_s, altitude h, and their respective first and second time
derivatives are identical, since the vehicle is directed along a radial path
to the beacon or landing site. The beacon antenna elevation angle ψ, meas-
ured from the lunar horizon, will also be constant at 90 deg throughout this
descent profile.

<p align="center">Table 3-1. Vehicle Parameters for Direct Radial Approach</p>

Initial weight before burn	79,400 lb (Earth weight)
Thrust	30,000 lb
I_{sp}	440 sec
Trajectory	72-hour flight time on radial path
Start of burn	Altitude of 744 km at 584 sec before time of final position
Final position	Altitude of 305 meters with velocity of 9.1 m/sec and acceleration of 5.9 m/sec^2
Pitch maneuvers	None

Figure 3-1 shows the pertinent ranges of R, R_s, h, and their respective
velocities and accelerations for the direct-approach landing with no beacon
offset. (Time is measured negatively from final position in all figures.)
The positive direction of velocity and acceleration is taken as away from
the center of the Moon. However, to simplify the plotting, negative values
of all velocities are graphed. For this profile, the angle requirements are
minimum since all angle velocities and rates are zero. The angular cover-
age required does not exceed either the 110 by 60 degrees for the beacon-
assisted descent or the 60 by 60 degrees for the non-beacon-assisted descent
presented in Int. Rept 1. The only sensor performance parameters that
penetrate the envelope of sensor requirements enumerated in Int. Rept 1
are those for maximum range and altitude, both being 744 km, thus exceed-
ing the original estimate of 700 km. However, the decrease in signal level
due to operation at the higher altitude is only 0.5 db and can be neglected
in any assessment of performance.

---

[*] Slant range, R_s, of the Slant Range Tracker-Velocity Meter is measured
along the axis of the antenna assembly to its intersection with the lunar
terrain. The orientation of R_s is taken to be colinear with the vehicle's
longitudinal axis. The range to the beacon from the spacecraft is given
by R. A switching of sensors is effected at R_s = 10 km for the non-beacon-
assisted cases. Above 10 km, an altimeter is employed; whereas below
10 km, a slant range tracker and velocity meter is used.

FIGURE 3-1 DIRECT APPROACH ALTITUDE AND SLANT RANGE FOR BOTH OFFSET AND NON-OFFSET BEACON AND BEACON RANGE FOR NON-OFFSET BEACON; AND RESPECTIVE DERIVATIVES
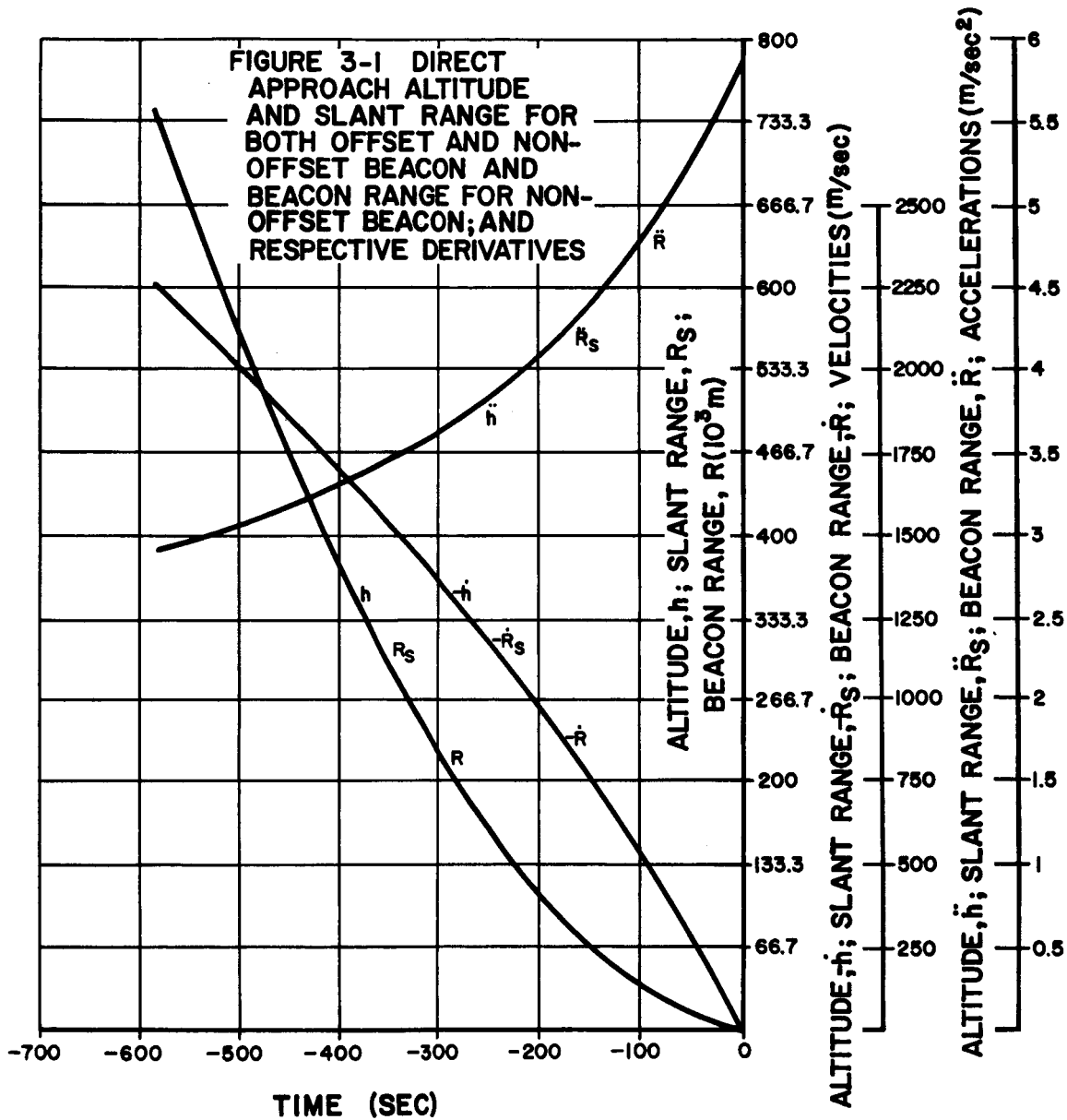
The discrepancy between this calculation of the maximum altitude and the earlier calculated value can be attributed to the different assumptions made. Although the presently considered Multimission Module is heavier, the previous model of the Multimission Module had two stages and hence jettisoned a portion of its weight subsequent to initial burning. The I_{sp} for

3-3

the previously considered vehicle was lower and therefore more fuel was consumed (because each of the vehicles have the same thrust) which decreased the weight more rapidly, permitting deceleration at a higher rate. Lastly, a constant value of lunar gravity was assumed for the prior estimate, and the actual value of gravity was used in this calculation.

For the second type of direct-approach landing, i.e., at a landing site offset from the beacon by 9.3 km, the only parameters of the nonoffset direct-approach case affected by the offset are the angles between the LOS to the beacon, and the vehicle axis and the beacon range. Therefore, Figure 3-1 also shows the values of altitude and slant range, and their respective time derivatives for the beacon offset case. Figure 3-2 illustrates the beacon range R, and its time derivatives, and Figure 3-3 presents the beacon-elevation look angle, ψ.

As previously, all the position parameters and their time derivatives fall within the previously assigned sensor-performance envelopes, except for the maximum altitude and range. The rapid change in slope of $\ddot{R}$ near t = -100 sec arises because of the rotation of the line of sight (LOS) to the beacon. The rotation increases the angle between the thrust axis and the LOS, approaching 90 deg, as the spacecraft nears the landing site which more than compensates for the increase in the F/W ratio as fuel is consumed. The angle coverage specified in Int. Rept 1, 110 deg, is adequate if the axis possessing the larger gimbal freedom is oriented so as to contain the beacon and the vehicle's longitudinal axis. All angular rates are well within prior tolerances.

The beacon look angle, ψ, approaches the horizontal as the vehicle nears the landing site and a commanded switchover from the vertically directed beam to the diametrically opposed lobes oriented at 20 deg to the horizontal would be made at about 45 deg from the vertical. Multipath constraints impose a lower bound to the beacon antenna-elevation coverage. For the antenna coverage patterns of Int. Rept 1, 10 deg is appropriate. A beacon look angle of 10 deg is reached at an altitude of about 1.7 km for the 9.3-km offset. The quality of the range and the angle data would be compromised at lower altitudes (see Section 4). For guidance to lower altitudes, it would

FIGURE 3-2 DIRECT APPROACH BEACON RANGE AND DERIVATIVES FOR OFFSET BEACON
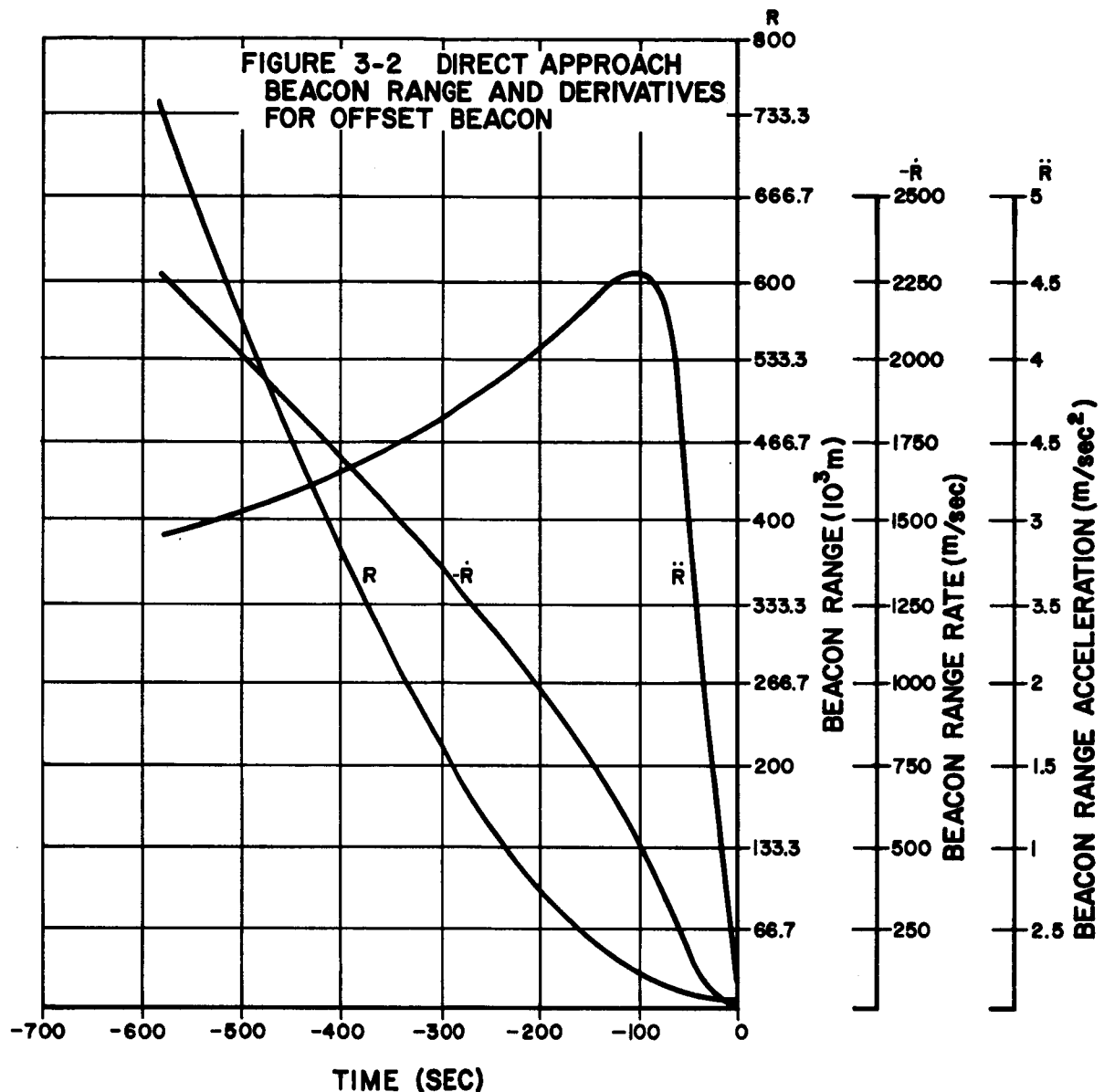
be necessary to utilize the IMU and an altimeter, the latter being required if terrain irregularities were unknown in the vicinity of the landing area. A fuller discussion of these points is presented in Int. Rept 1..

In summary, for both the offset and nonoffset cases of a direct radial descent of the Multimission Module, the sensor performance parameters as stated in Int. Rept 1 will be sufficient except for the maximum altitude and range, which should increase to 800 km.

3-5

FIGURE 3-3 DIRECT APPROACH
BEACON LOOK ANGLE FOR
OFFSET BEACON
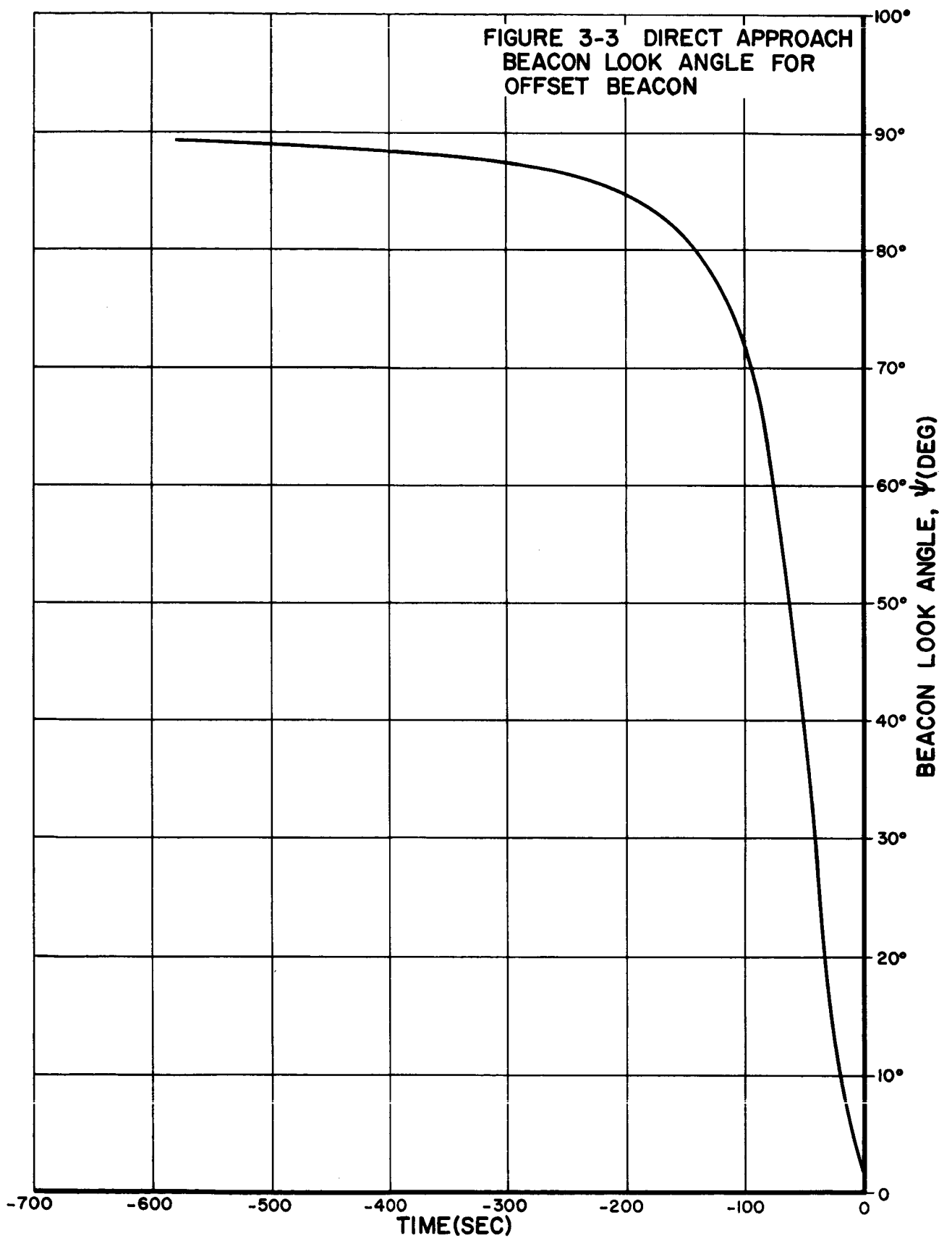
3.2 Multimission Module on Orbital Descent

The specifications employed to determine the orbital descent trajectory are shown in Table 3-2. As in the direct descent, two cases were considered: the first a landing on the emplaced beacon and the second a landing 9.3 km downrange of the emplaced beacon. The only changes to the trajectory parameters of the nonoffset case incurred by offsetting the beacon from the landing site will be in the values of range and its derivatives and the angle subtended between the beacon and the vehicle axis.

Table 3-2. Orbital Descent of a Multimission Module

Initial weight before burn	67,500 lb (Earth weight)
Thrust	30,000 lb
I_{sp}	440 sec
Trajectory	Hohmann transfer from 148 to 15 km
Start of burn	Altitude of 15 km
Final position	Altitude of 305 meters with velocity of 0.03 m/sec and acceleration of 5.0 m/sec^2.
Pitch maneuvers	Constant pitch rate of 0.12 deg/sec after start of burn until 2 sec from the final position, at which time an instantaneous pitch of 63.50 deg is executed.

For the nonoffset case of the orbital descent, Figures 3-4, 3-5, and 3-6 show the altitude h, slant range R_s, and beacon range R, respectively, along with their respective velocities and accelerations. Main braking from the transfer ellipse occurs at t = -330 seconds, which results in the altitude acceleration becoming negative in Figure 3-4. The decrease in $\ddot{R}$ shown in Figure 3-6 near t = -40 seconds arises because the vehicle is pitching at a rate of 0.12 deg/sec for $|t| < 40$ seconds and the rate of rotation of the LOS is increasing rapidly so that the thrust axis no longer coincides with the LOS to the beacon. However, for $|t| > 40$ seconds, the vehicle longitudinal axis remains pointed within 4 deg of the beacon landing site, and hence $\ddot{R}$ increases with F/W as fuel is expended. The beacon look angle,

h

ḧ

−3800   −3600   −3400   −3200   −3000   −2800   −2600   −2400   −2200   −2000   −1800   −1600

TIME(SEC)

FIGURE 3-4 ORBITAL DESCENT ALTITUDE AND DERIVATIVES FOR BOTH OFFSET AND NON-OFFSET BEACON

3-8

FIGURE 3-5 ORBITAL DESCENT SLANT RANGE AND DERIVATIVES FOR BOTH OFFSET AND NON-OFFSET BEACON

FIGURE 3-6 ORBITAL DESCENT BEACON RANGE & DERIVATIVES FOR NON-OFFSET BEACON
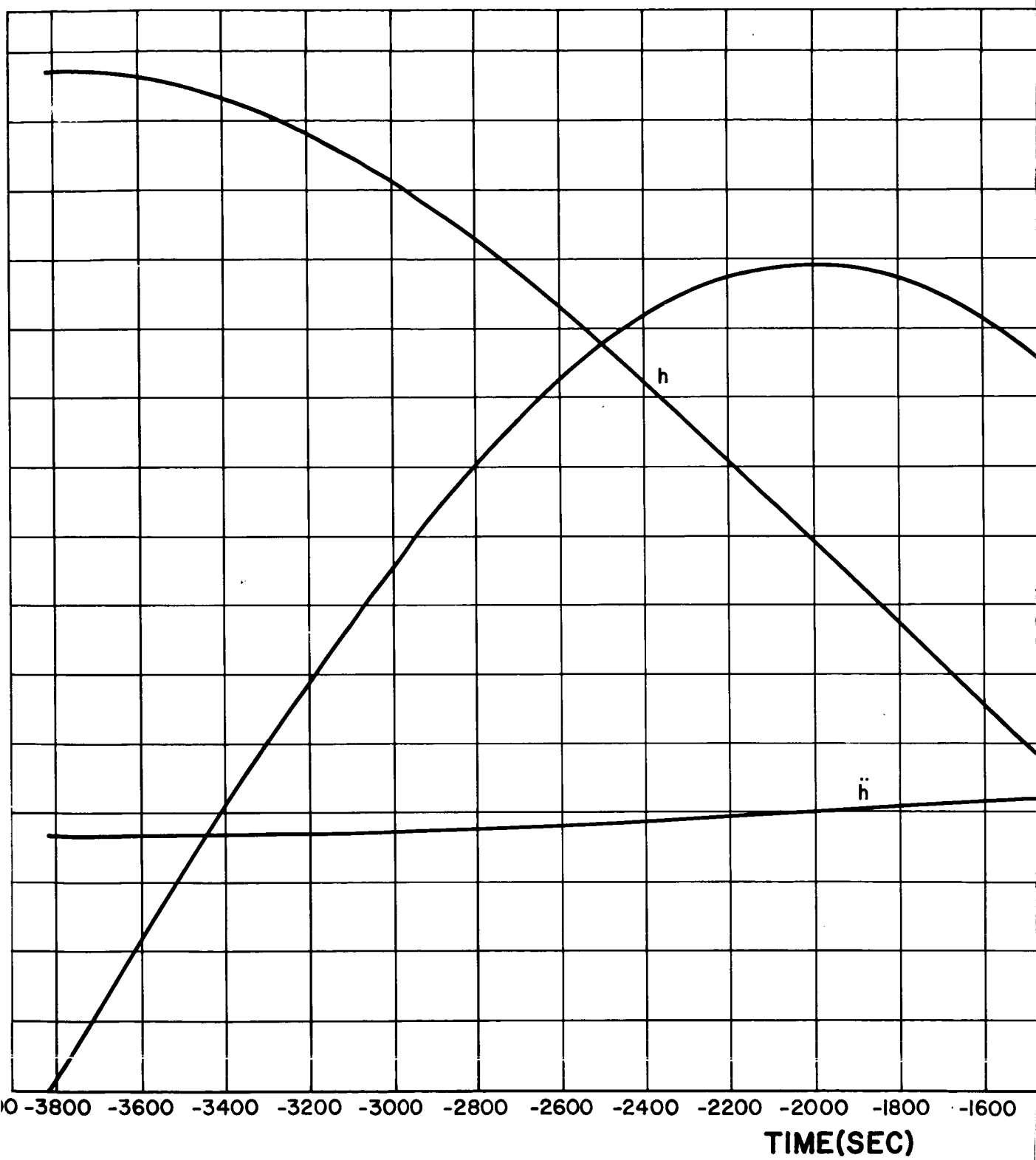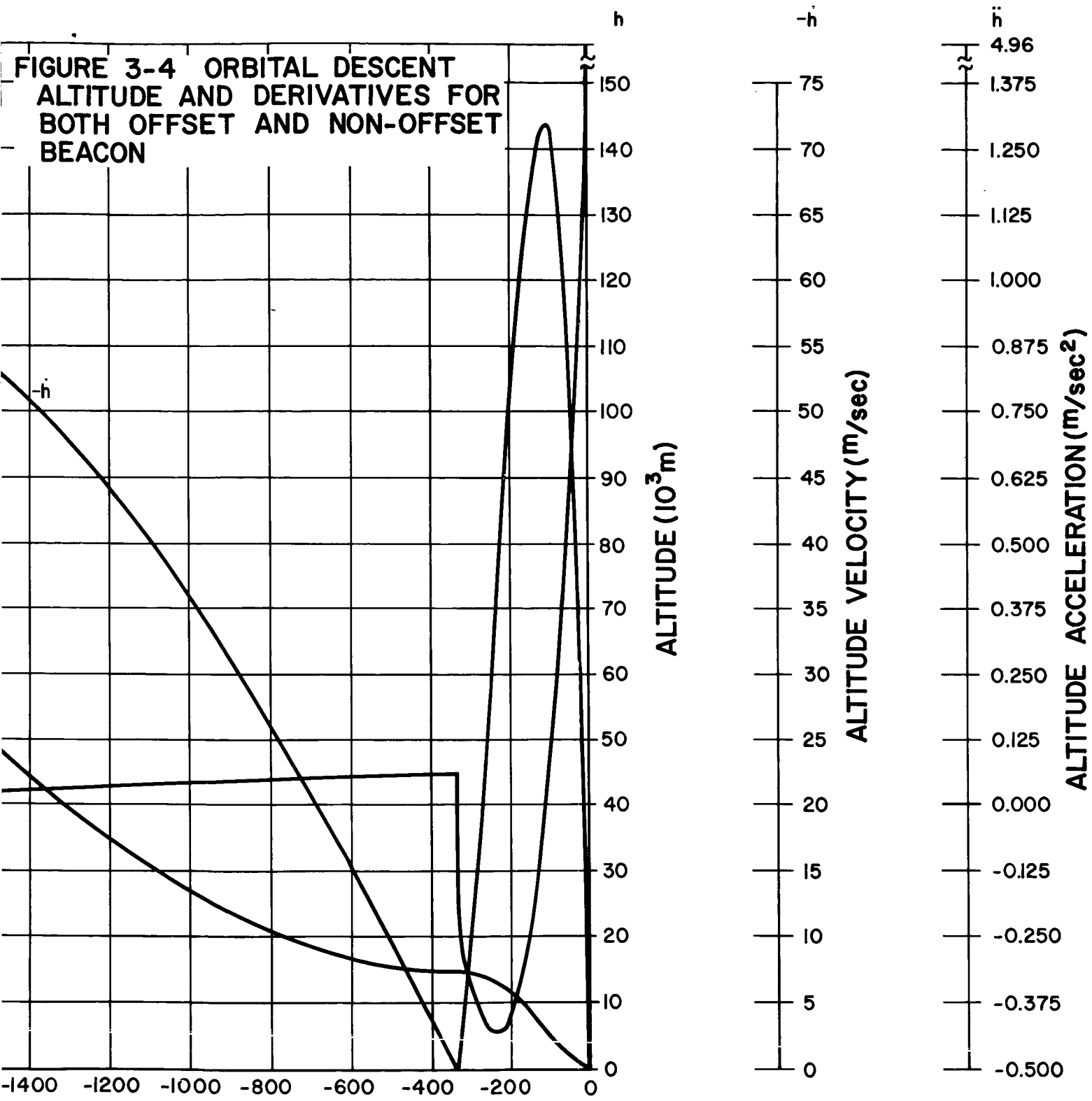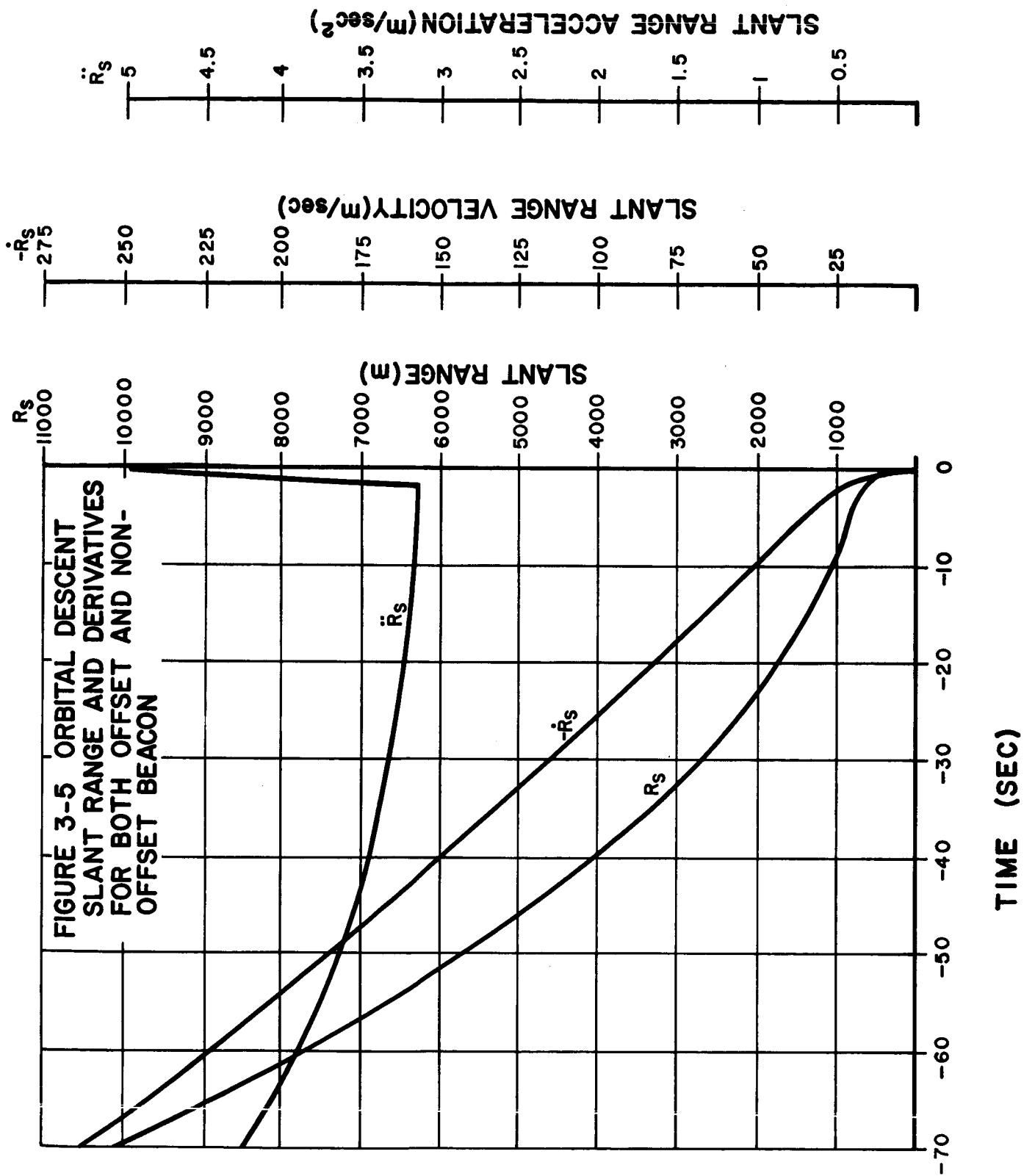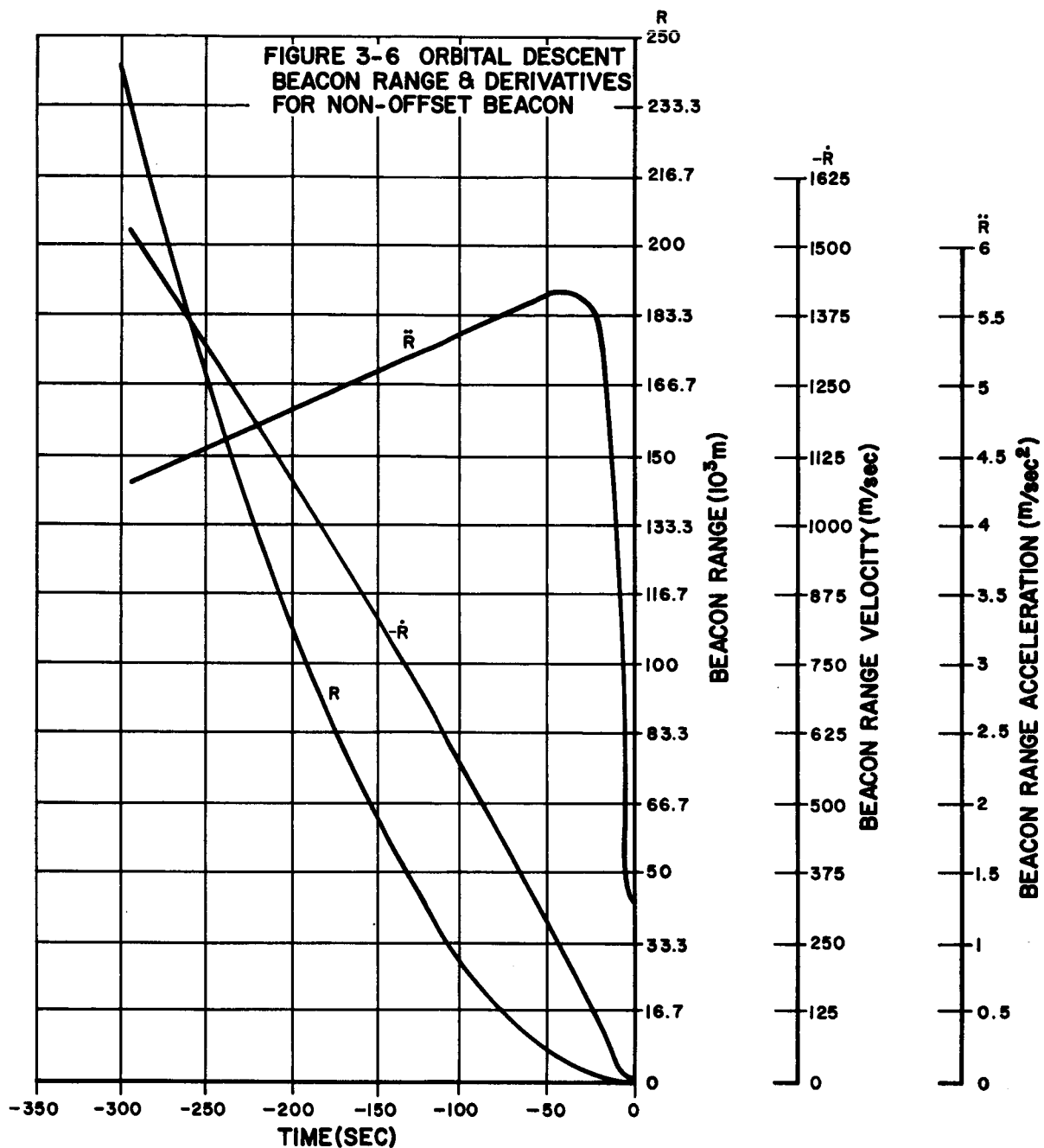
ψ, is shown in Figure 3-7. Because of the shallowness of the reference trajectory, ψ does not exceed 10 deg until the range, R, is 28 km. Either a steeper trajectory must be flown for beacon-assisted descents, or multiple beacons must be deployed along or near the projection of the descent profile upon the lunar surface, as guidance information is required at longer ranges.

FIGURE 3-7 ORBITAL DESCENT
BEACON LOOK ANGLE FOR
NON-OFFSET BEACON

3-11
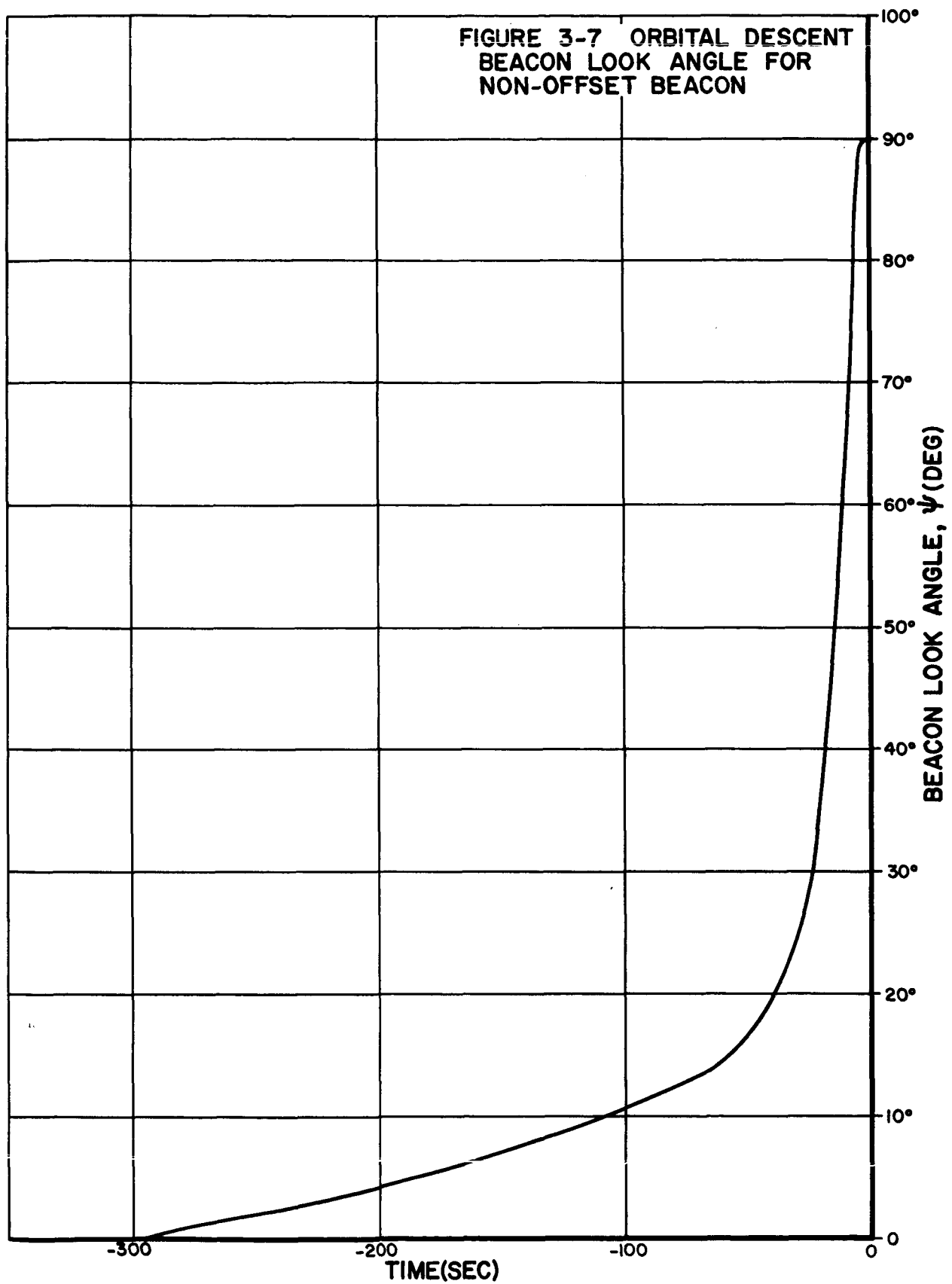
Two sensor performance parameters exceed the prior estimate for this case. They are the angle from the vertical required in the Slant Range Tracker-Velocity Meter for the non-beacon-assisted descents and the vehicle angle rate required for the beacon-assisted descents.

During the terminal phase of the descent profile, the vehicle longitudinal axis is within approximately 25 deg of the local horizontal. The pitch maneuver executed near touchdown consists of a very low pitch rate, 0.12 deg/sec, in conjunction with a large step in pitch 2 sec before assumption of final position to orient the vehicle in vertical position for landing.[*] The large horizontal component of velocity can be efficiently removed in this manner. As a result, the axis of the Slant Ranger Tracker-Velocity Meter exceeds the envelope of 0 to 45 deg from local vertical specified in Int. Rept 1.

In addition, the large pitch rate near touchdown causes the vehicle angle rate to exceed 6 deg/sec. As stated in Table 3-2, an instantaneous pitch of 63.50 deg was assumed 2 sec before the final position was reached to simplify the computations. In an actual landing, this pitch change would be smoothed out by proper shaping of the terminal portion of the descent profile. In fact, implementation of pitch rates greater than 6 deg/sec is not to be expected, and it would appear that the vehicle angle rate specification of 6 deg/sec would more than encompass any actual trajectory requirements.

For the beacon offset case, as stated previously, the altitudes and slant ranges, and their respective derivatives, for both the beacon offset and nonoffset cases are equal and, therefore, Figures 3-4 and 3-5 are applicable to both cases. Figure 3-8 shows the beacon range R and its velocity and acceleration, and Figure 3-9 shows the beacon look angle for the offset case. The same comment as made above with respect to Figure 3-6 is appropriate with respect to the drastic change in the slope of $\ddot{R}$ now occurring near t = -80 sec. $\dot{R}$ reverses polarity near t = -60 sec as the beacon is overflown.

---

[*] This large pitch maneuver causes the apparent discontinuities at the end of some of the figures. For example, the range acceleration, $\ddot{R}_s$, in Figure 3-5 experiences a large transient due to this cause 2 seconds prior to the final position.

FIGURE 3-8 ORBITAL DESCENT BEACON RANGE AND DERIVATIVES FOR OFFSET BEACON
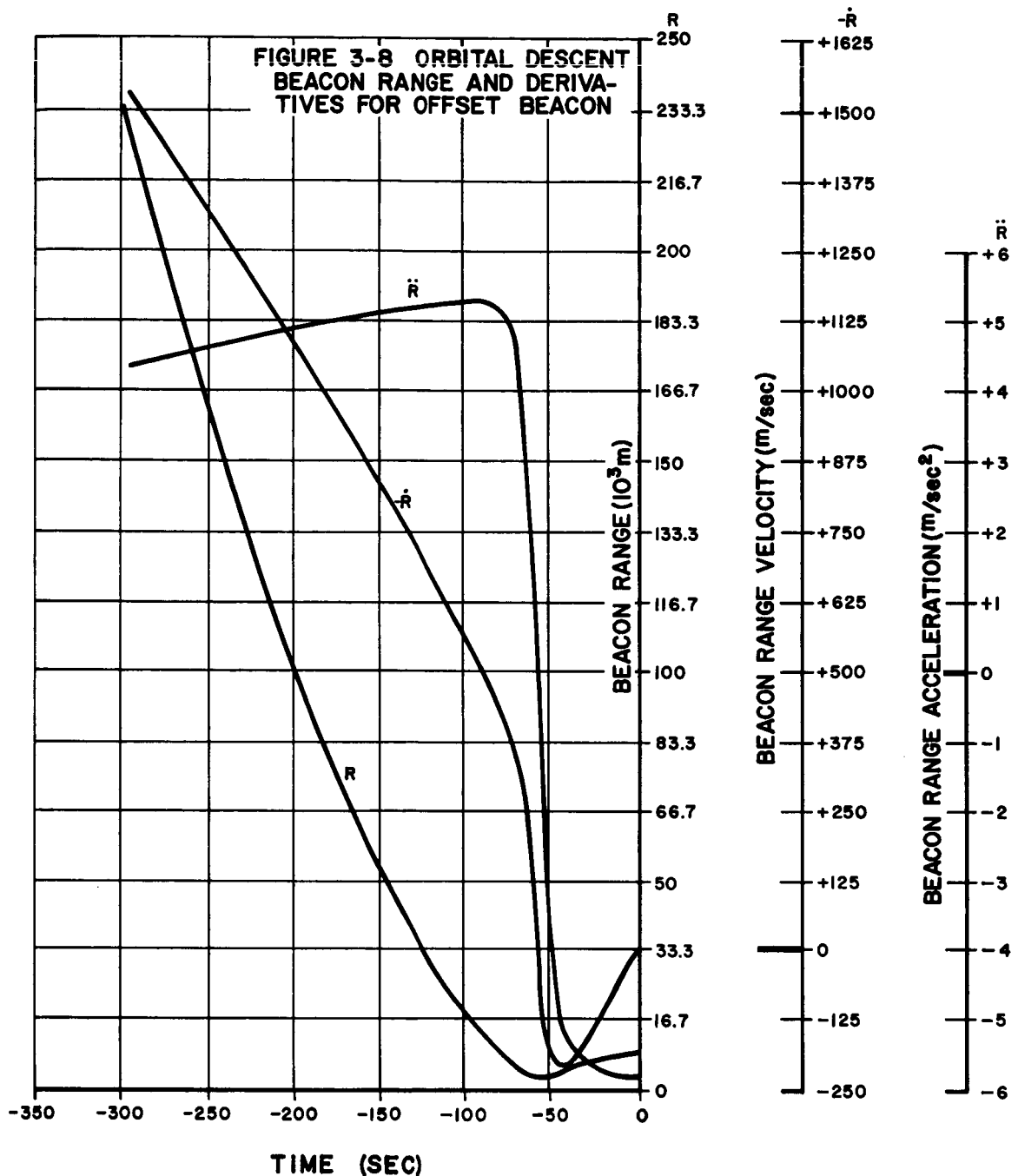
The comments pertaining to the look angle measured from the local vertical and the vehicle angle rate apply also to the beacon-assisted offset landing. In addition, the following sensor performance parameters are exceeded: the radar antenna angular coverage for the beacon-assisted descent, the beacon range acceleration, and the inertial angular rate. The beacon range acceleration has a minimum of -5.8 m/sec^2 due to a downrange

3-13

FIGURE 3-9 ORBITAL DESCENT BEACON LOOK ANGLE FOR OFFSET BEACON
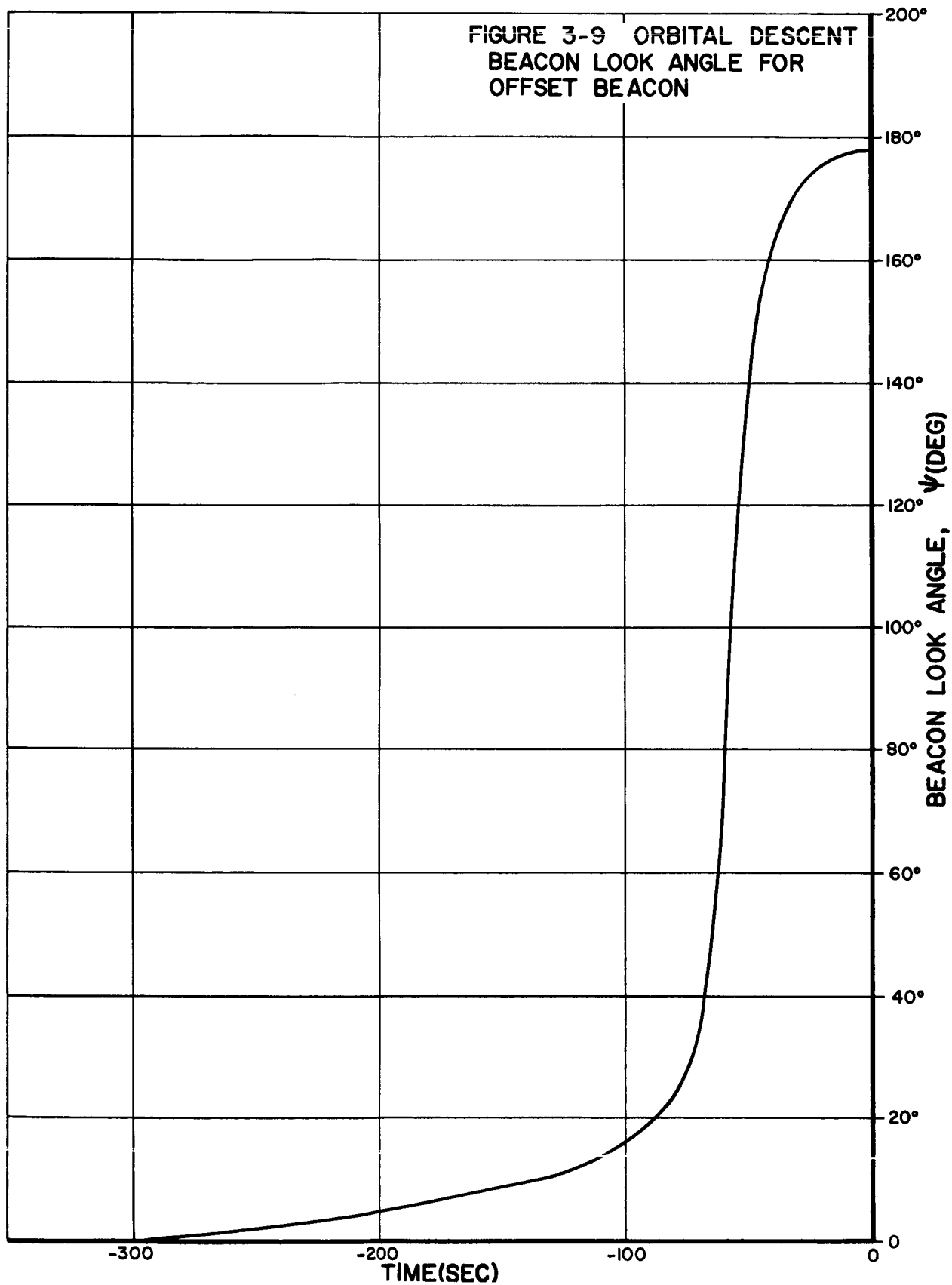
landing rather than the specified 0.0 m/sec^2. Therefore, a change to a requirement of from -8 m/sec^2 to the previous maximum of 27 m/sec^2 is sufficient to handle any trajectory considered to date. The inertial angular rate has a maximum of 6.3 deg/sec as the vehicle passes over the beacon, and this rate exceeds the specified 6 deg/sec. An increase to an inertial angular rate of 8 deg/sec is indicated.

The most serious excursion from the previous sensor performance requirements is in the angular coverage required for the beacon-assisted descent when the beacon is offset from the landing site. For the reference trajectory used, the angle changes over 150 deg compared to the specified 110 deg. The reason for the large change is again due to the vehicle's attitude being maintained within approximately 25 deg of the horizontal until near touchdown. This causes a large change in the vehicle look angle: a measure of the antenna gimbal freedom needed. If an increased pitch rate were used prior to arrival at the final position, such as 1 or 2 deg/sec, a significant decrease in the angular coverage needed could be achieved.

An increase in the gimbal freedom requirement for the beacon tracking antenna would accommodate this increased angular coverage. This solution would not present unreasonable problems of implementation for the sensor design. A second alternative consists of achieving a decrease in the angular coverage volume by using a higher approach altitude and hence a steeper pitch angle. As mentioned earlier, some trajectory modification of this type is needed in an actual situation to eliminate the large step change in attitude present in the simplified trajectory used for this analysis. An increase in fuel consumption results, however, in comparison to the shallower trajectory. A more complete discussion of the indicated STELATRAC modifications is presented in Section 4 for the somewhat pessimistic requirement of 150-deg pitch angular coverage.

In summary, for the orbital descent of the Multimission Module, changes in the sensor performance parameters for the beacon range acceleration and the inertial angular rate are easily accommodated. The problems involved with the radar antenna angular coverage and the associated solutions are discussed in the section on modifications.

3.3 Discussion of Sensors for Other Mission Phases

In addition to providing guidance for consumating the soft landing, RF sensors are useful for other mission phases. Obvious examples are sensors for braking into lunar orbit from an Earth-Moon transit trajectory, rendezvousing with other spacecraft in orbit about the Earth or Moon, etc.

For the former application, a velocity meter is extremely useful to establish velocity in and transverse to the desired orbit plane (if the DSIF is not tracking the spacecraft) so that the proper time of thrust initiation and the appropriate vehicle attitude can be obtained when braking into lunar orbit. Typically, velocity measurements are desired from altitudes up to 450 km and down to the orbital altitude of 185 km. Such a requirement is not commensurate currently with solid-state operation at X-band with a 60-cm antenna aperture. By reducing the frequency of operation to S-band, and by employing low-noise RF amplifiers in each channel and an antenna aperture 1 meter in extent, such a capability is feasible in the near future if the vehicle can be steered to properly position the antenna assembly so that a minimum loss in the lunar scattered return is experienced. This steering and positioning would be feasible in most instances as the spacecraft is in free flight. The development of such a sensor with the requisite performance would permit injection into lunar orbit on the other side of the Moon, outside of the DSIF contact.

An altimeter is not quite as useful for the same application since it measures altitude and altitude rate, and these must be converted into velocities along the flight path. Such a transformation gives rise to large error coefficients. Needless to say, an altimeter with the design features possessed by the Extended Range Altimeter can operate to 750 km with the same assumptions as used above with the velocity meter. There is no longer a three-way splitting loss as occurs with the velocity meter. An altitude accuracy of 0.5 percent or less is desired, to be competitive with other devices.

Lastly, rendezvous with logistics and other spacecraft can be readily established by placing the beacon on the target vehicle. A range capability to 1,850 km can be readily provided. STELATRAC was initially conceived and developed for such applications and possesses the versatility to fulfill

3-16

many combinations of requirements. The requirements enumerated in
Table 2-2 are representative for many rendezvous- and docking-mission
profiles.

4. STELATRAC MODIFICATIONS

During the initial phase of the work performed on NAS8-5205, an enve-
lope of sensor requirements was evolved for both beacon and non-beacon-
assisted descents. The Multimission Module, when flown on representative
orbital descent profiles, causes the prior envelopes to be significantly
exceeded in two parameters. These are the pitch-axis gimbal freedom
required of the beacon tracker, and the angle between the axis of the Slant
Range Tracker-Velocity Meter antenna and local vertical. These two
parameters are discussed more fully in the following subsections.

4.1 Beacon-Tracker Angular Coverage

A shallow orbital descent trajectory conserves fuel by orienting
the thrust vector more nearly colinear with the horizontal velocity compon-
ent during most of the terminal thrusting phase. To properly orient the
vehicle just prior to assuming final position, a rapid pitch maneuver is
programmed. As a result, the radar LOS to the beacon goes through a
large angular excursion when the Multimission Module overflies the im-
planted beacon. Angular coverage volumes in the pitch plane of up to 150
deg can be experienced in this instance. It is recalled that the gimbal free-
dom in the pitch plane was specified at 110 deg in Int. Rept 1. Fortunately,
this can be increased to 150 deg with little additional penalty in moment-of-
inertia, weight, or performance for antenna apertures measuring 60 cm or
less in extent. The out-of-plane coverage can be maintained with a gimbal
freedom of ±30 deg in conjunction with a minimum acceptable elevation angle
of 10 deg as viewed from the beacon if the vehicle's roll attitude can be
varied to accommodate the particular touchdown geometry. Many airborne
intercept (AI) antennas have gimbal freedoms of 140 deg in both axes and
require angular scan rates up to 100 deg/sec to encompass the search sector.
The search sector appropriate to the lunar landing mission is representable
by a 7 deg, half-angle, conical volume. (A coverage volume measuring less
than 7 deg half angle in the plane of descent would be adequate.) Scan speeds
of 15 deg/sec are acceptable. As a result of the low scan speeds, the
angular acceleration is reduced in relation to that of AI antennas so that the
increase in the moment-of-inertia attributable to the larger angular coverage
does not require excessive torques. Depending upon the antenna pedestal

design, the increased coverage may be obtained by tilting the pedestal, making a cutout in the planar array to prevent mechanical interference when the antenna is depressed, as well as by using a longer lever arm in the pitch coordinate. The former two alternates cause little or no increase in weight. In any event, the additional weight penalty incurred by the enlarged gimbal freedom requirement will not exceed 3 pounds. Needless to say, 3 pounds of fuel will provide a very small acceleration increment to make up for the inefficiencies of a steeper descent profile which would negate the need for wide angular coverage.

However, since the sensor data quality is degraded for beacon-elevation look angles measuring less than 10 deg, and as guidance data are required for R > 28 or 38 km for the nonoffset and offset landings, respectively, it is evident that a somewhat steeper trajectory than used in the trajectory study must be flown, and hence the gimbal freedom in the pitch plane can be reduced below 150 deg. From a prior study[*], STL determined that a gimbal freedom of 120 deg in the pitch plane would be adequate. The optimum gimbal freedom requirement in the pitch plane is therefore somewhere between 120 and 150 deg.

4.2 Beacon Antenna Coverage

For a nonoffset landing from lunar orbit, the beacon antenna elevation angle does not exceed 10 deg until approximately 100 sec before touchdown. At this time the range between the incoming spacecraft and the emplaced beacon is about 28 km. For orbital descent to a landing site offset 9.3 km downrange from the beacon, the corresponding range is 38 km.

Thus a minimum elevation angle of 10 deg restricts the achievement of full sensor accuracy in the range and angle coordinates to ranges of 28 and 38 km for nonoffset and offset landings, respectively. The denial of accurate sensor data at lower elevation angles degrades the utility of such shallow descents when beacon-assisted. For a reasonably flat landing site and with

---

[*] "Study of Spacecraft Bus for Lunar Logistic System," Vol I, "Summary," 8689-6007-TU-000, Space Technology Laboratories, Inc., 22 December 1962.

no local obstructions in the LOS, the beacon antenna lobe of 30 deg half-power-beamwidth oriented approximately 20 deg above the horizontal will have a null in its radiation pattern at about the aspect from which specular reflection would be directed to the descending spacecraft. Fortunately, the lunar scattering coefficient is depressed in this region, being of the order of -20 to -30 db relative to its value at vertical incidence. (See Section 4.4.2 of Interim Report No. 1.) For a multipath signal 25 db down from the direct ray, the maximum phase shift in the ranging sideband is ±6.5 deg. As the conversion factor for the coarse range mode is 2.8 m/deg, the multipath signal can result in a range error of 18.3 meters, which is about the total ambiguity resolution interval of the coarse range mode. Thus the range accuracy is impaired until the elevation angle increases about 10 deg. However, it should be pointed out that the percentage range error is still under 0.1 percent (more than adequate for guidance purposes). The slope of the beacon elevation angle versus range steepens fairly rapidly as the range shortens, so that the ambiguity interval can be resolved by the time it represents an appreciable fraction of the range interval, i.e., 0.5 percent. Conversely, a doubling of range will approximately halve the elevation angle for an offset landing and reduce it to about 7 deg for the nonoffset landing. But now, maria slopes of 3 to 5 deg and reflections from other vehicles in the nearby vicinity become significant. As these factors are difficult to determine analytically, a minimum obscuration angle of 10 deg is recommended.

The radar antenna must be placed on the Multimission Module so that it can look through the longitudinal axis of the vehicle by approximately 5 deg and have sufficient visibility about the landing legs. It was shown in Interim Report No. 1 that flame effects from two RL-10A engines are negligible at X-band, even when looking through the exhaust.

4.3 Slant Range Tracker-Velocity Meter Incidence Angle (SRT-VM)

It is recalled that the SRT-VM antennas in Interim Report No. 1 were body-mounted to eliminate any requirement for gimbaling. However, due to the shallowness of the orbital descent profile and the resulting vehicle attitude, this approach is no longer feasible as the vehicle axis makes an angle with the local vertical in excess of 70 deg during periods of thrust.

For orbital descent via a Hohmann transfer, it is not economical of fuel to use a descent profile where the above angle is maintained less than 45 deg for slant ranges of 10 km and less, i.e., the range at which operation of the SRT-VM occurs. For this reason, it is believed necessary to gimbal the three antenna apertures in one plane between two discrete steps so that the axis of the SRT-VM antenna assembly never deviates farther than 45 deg from the local vertical, and the largest deviation occurs at maximum range where accuracy requirements are more relaxed. At and near touchdown, where accuracy of the measurement is critical, the deviation from vertical would be very much less. The antenna assembly would be driven between detents so as to ensure accuracy of alignment to 0.5 deg[*]. Drive would be effected via a torque motor assembly. A rotation of 40 deg would require about 4 sec to complete. This time period is not excessive, and it could be shortened if a preloaded spring were used to rotate the antenna assembly. The weight increase attributable to such an arrangement would be 4 pounds.

---

[*] It is shown in Interim Report No. 1 that an antenna alignment error of 0.5 deg causes a 3-σ velocity error in the slant range channel of 0.4 percent and in the two offset channels of 0.16 percent.

5. DYNAMIC SIMULATION OF ALTITUDE TRACKER

The purpose of the dynamic simulation of the altitude tracking loop was to study the effects of variations in loop gain, bandwidth, and performance parameters over the operational dynamic ranges of altitude, velocity, and acceleration. The altitude tracking loop was investigated on a hybrid analog-digital simulation facility. The hybrid simulation was utilized in preference to a pure analog implementation as the hybrid simulation permitted ready insertion of the altitude profile data from the trajectory study of Section 3, and also increased the accuracy of the simulation results. The analog portion provided an on-line facility for ready examination of the results when varying parameter values. The dynamic ranges of operation were obtained from three different typical trajectory profiles consisting of the Multimission Module on a direct descent, the Multimission Module on an orbital descent, and a test case descent to define the performance of the tracker when perturbed by acceleration steps. The error in the altitude indicated by the tracker was then found with and without a noise disturbance introduced in the loop. The output data were presented in graphical form.

5.1 Implementation

The implementation of the altitude tracker was initiated from the altitude tracking loop model shown in Figure 5-1, which is essentially the model presented and discussed in Interim Report No. 1, Section 4.2.2.1. The specific objects of this study were: to select values for the parameters T_1, T_2, T_3, and K_v defined in Figure 5-1; determine the equivalent loop noise bandwidth, B_N; and quantitize the errors resulting from the chosen parameter values, based on actual altitude profiles.

Figure 5-2 is a simplified block diagram of the hybrid analog-digital computer and defines the terms used. The actual working flow diagrams and analog block diagrams are shown in Appendix A as Figures A-1, A-2, and A-3. In the actual altitude tracking loop, phase changes introduced by time delay will produce the altitude measured. For the purpose of simulation, altitudes were used explicitly as the variables instead of the phase angles in the loop operation. This is allowed, since, as shown in Figure 5-1, the time delay, τ, is related to the altitude by a multiplicative constant.
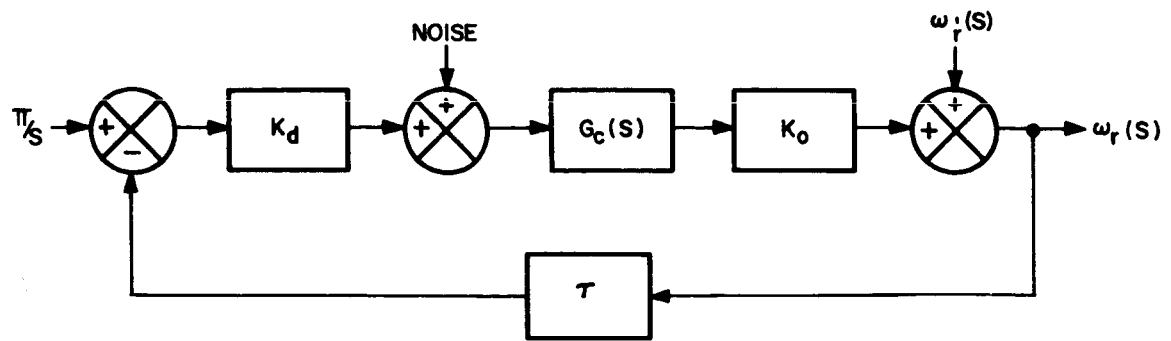
FIGURE 5-1. ALTITUDE TRACKING LOOP MODEL

K_d = ERROR DETECTOR CONSTANT $[\text{VOLT/RAD}]$

K_0 = SCALE FACTOR OF PRF VCO $[(\text{RAD/SEC})/\text{VOLT}]$

τ = TIME DELAY IN PROPAGATION PATH *

$\quad (= \dfrac{2h}{C}$, h = ALTITUDE, C = VELOCITY OF PROPAGATION)

$G_c(S) = \dfrac{K_c(T_2 S+1)}{(T_3 S+1)(K_c T_1 S+1)}$, COMPENSATION NETWORK

$\quad$ WITH K_c = DC GAIN OF INTEGRATING AMPLIFIER

$\qquad\quad T_2$ = LEAD TIME CONSTANT

$\qquad\quad T_3, K_c T$ = INTEGRATION TIME CONSTANTS OF COMPENSATOR

$K_v = K_d K_c K_0 \tau$ = OPEN LOOP GAIN

ω_r^i = REST FREQUENCY OF PRF VCO

ω_r = ALTITUDE TRACKER OUTPUT

Discrete altitudes as functions of time from the three descent pro-
files were introduced into a digital computer and quadratically interpolated
to give an approximation to the continuous altitude changes. The altitude
from the analog tracker loop was then sampled and a loop tracking error,
referenced to the actual altitude used in the descent profile, was computed
in the digital computer, and subsequently converted back to analog data.

The loop tracking error was then processed in the analog computer
through the compensation network to produce a tracking loop altitude from

---

* A gain factor slowly varying with respect to loop response characteristics
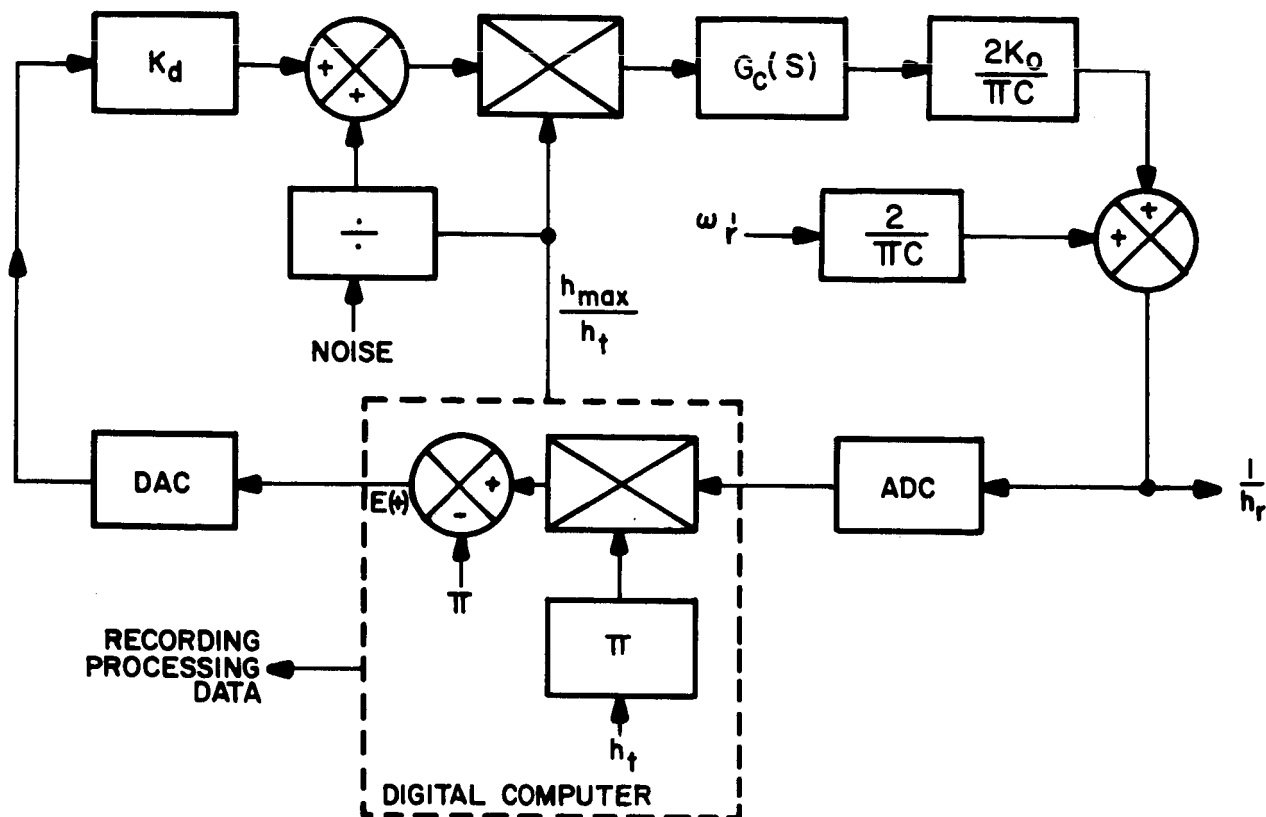
K_d = ERROR DETECTOR CONSTANT $\left[\text{VOLT/RAD}\right]$

$G_c(S)$ = COMPENSATION NETWORK $\left[\text{DEFINED IN FIGURE 5-1}\right]$

K_o = SCALE FACTOR OF PRF VCO $\left[\text{(RAD/SEC)/VOLT}\right]$

C = VELOCITY OF PROPAGATION

ω_r' = REST FREQUENCY OF PRF VCO

ADC = ANALOG TO DIGITAL CONVERTER

h_t = PROFILE ALTITUDE

h_r = TRACKER ALTITUDE

h_{max} = MAXIMUM ALTITUDE AT START OF PROFILE

DAC = DIGITAL TO ANALOG CONVERTER

$E(t) = \pi \dfrac{h_t - h_r}{h_r}$, TRACKING LOOP ERROR

FIGURE 5-2. COMPUTER SIMULATION

which a new tracking loop error was computed, etc. An output from the digital computer was provided for recording the actual tracking loop altitude error from the profile altitude and for use as gain compensation in the tracking loop. Gain compensation was achieved by feeding back, effectively, the actual altitude rather than the tracking loop altitude. It was believed, with regard to the implementation of the gain compensation, that the small tracking errors found allowed the use of the actual altitude rather than the loop altitude. In an implementation of the altitude tracking loop, gain compensation would be accomplished by feeding back the loop output.

Noise was introduced in the tracking loop as shown in Figure 5-2. Instrumentation difficulty was encountered, however, which allowed the employment of only a quarter of the full noise power spectral density. The reason for this difficulty lay in the fact that a completely new scaling change would have to be accomplished throughout the analog portion of the simulation to accommodate the full noise power spectral density, and it was believed that this was unwarranted. To confirm this hypothesis, test runs were made on the simulation, and it was ascertained that the tracking loop behaved in a linear manner with respect to the noise input.

Data on the operation of the altitude tracker were obtained from three basic profiles: the Multimission Module on a direct radial descent; the Multimission Module on an orbital descent; and a test case descent. The first two altitude profiles were altitude versus time data taken from Sections 3.1 and 3.2 of this report. The test case profile was a hypothetical descent which used alternating periods of thrust and freefall to accomplish the landing. In addition, increments in velocity were inserted at the origin of each region. The basic purpose of this latter profile was to evaluate the tracker under the transient conditions of the acceleration bursts required for descent and permit a numerical comparison with the analysis in Interim Report No. 1. The two Multimission Module profiles, on the other hand, represent more realistic descent conditions.

The operational data from the altitude tracking loop simulation study consists of the percent error of the tracking loop altitude function measured relative to the actual profile altitude. The percent error was expressed as

5-4

both an average error and rms error, using an averaging period of 10 seconds, and plotted directly from the simulator as a function of time, or, equivalently, altitude.

To accommodate the large dynamic range of altitudes, the two Multimission Module descent profiles were divided into three altitude regions, and the test case profile was divided into four altitude regions. Corresponding to each region of a particular altitude profile, specific values for the tracking loop parameters T_1, T_2, T_3, B_N, and K_v were determined to minimize the tracking error. The analog portion of the simulation was then set to the tracking loop parameters that had been specified for each altitude region prior to initiation of the run. Thus, a simulation of the tracking loop was achieved over the dynamic range of altitude encountered. Although the implementation seems unorthodox when compared to conventional analog-type solutions, it has the appearance of being a straightforward extension of conventional methods. The appearance of being an extension of conventional methods proved to be an unwarranted assumption, however.

The basic technical problem area lay in the interface region between the digital and analog computers. The major cause for this problem was the large dynamic range of altitudes encountered which resulted in the division of the altitude profiles into discrete regions. At the junction of the regions, certain scaling changes were made, as well as changes in the parameters of the compensation network. These modifications required certain initial conditions to be inserted at the start of each region after the first region. Because of the scaling changes in going from one region to the next, bits were lost in the analog-to-digital converter. The loss resulted in a quantization error in the initial condition transfer. The error arising from the transfer of initial conditions is noticeable at the interface between altitude regions, but does not negate the utility of the simulation in estimating the performance characteristics of the altitude tracking loop.

Another problem associated with the interface between the digital and analog computers was the small percentage changes occurring in the altitude profile at the high altitudes. Because of the small magnitude of the change, a small error incurred in the sampling when going from the analog-to-digital portions of the simulation resulted in a large error in the tracking

loop error function as determined by the digital computer. This error was reduced by quantitizing the changes in the output of the tracking loop, and then sampling the change in the loop output. Thus, a satisfactory solution was accomplished.

5.2 Results

The results of the simulation of the altitude tracking loop, both in the presence and absence of noise, are presented in the form of graphs. These graphs, plotted as a function of altitude, show both the average and rms error in percent of the altitude deviation of the tracking loop output from the profile altitude. As mentioned previously, only one-fourth of the expected noise power spectral density was used for the simulation because of scaling problems in the analog computer. Cognizance of this must be taken when examining plots containing a noise disturbance. Equation B-4 in Appendix B relates the plotted results to the values expected with the anticipated noise level. It was confirmed that the tracking loop response was linear with respect to the noise power, so that the errors with the full noise power disturbance can be readily determined. This has been done for the summary results given in Table 2-5.

It should be noted in the following graphs that apparent discontinuities exist at the junctions of the regions of the altitude profiles and at the beginning and the end of each run. These discontinuities can be attributed primarily to two factors: the previously mentioned interface problem between the digital and analog computers and the improvement in performance of the new compensation network parameters over the prior region network parameters. In addition, in the test-case descent, velocity steps were introduced at the origin of each region. The discontinuities at the limits of the graphs are functions of the simulation-processing of the data. It should be noted also that because of quantization and incidental analog-to-digital converter noise, the simulation errors for the rms plots where thermal noise is not dominant should not be read to an accuracy of less than 0.05 percent.

5.2.1 Orbital Descent Profile

The pertinent parameters for the orbital descent-profile altitude-tracking loop are shown in Table 5-1.

Table 5-1. Orbital Descent-Altitude Tracking Loop Parameters

Region	Altitudes (m)		Parameter Values				
	Maxi-mum	Mini-mum	B_N(cps)	T_1(sec)	T_2(sec)	T_3(sec)	K_v
1	147,000	14,870	0.3	7.9	2.5	80	2.2×10^5
2	14,870	1,688	1.0	0.73	0.75	80	2.2×10^5
3	1,688	338	3.0	0.33	0.25	10	2.2×10^5

Figure 5-3 shows the orbital descent-altitude profile. It was confirmed by use of this profile that improved performance could be achieved by using bandwidth switching, as can be observed from a comparison of the average errors plotted in Figures 5-4 and 5-5. In Figure 5-4 the same compensation network parameters were employed in all regions as were used in Region 1 for Figure 5-5. The improvement in error performance at low altitudes where the higher values of accelerations occur is quite noticeable. B_N in Figure 5-4 was selected for operation in Region 1, where noise errors predominate and is too narrow for operation at lower altitudes. Figures 5-5 and 5-6 show the average and rms errors in the absence of noise, respectively, while Figure 5-7 shows the rms error with noise present.

5.2.2   Vertical Descent Profile

Table 5-2 presents the pertinent tracking loop parameters for the vertical descent profile and the altitude profile for this case is shown in Figure 5-8. The average and rms errors with no noise disturbance are presented in Figures 5-9 and 5-10, respectively. The rms error with noise is shown in Figure 5-11.

Table 5-2. Vertical Descent-Altitude Tracking Loop Parameters

Region	Altitudes (m)		Parameter Values				
	Maxi-mum	Mini-mum	B_N(cps)	T_1(sec)	T_2(sec)	T_3(sec)	K_v
1	264,000	16,570	0.3	7.9	2.5	80	2.2×10^5
2	16,570	1,640	1.0	1.32	0.75	80	2.2×10^5
3	1,640	305	3.0	0.59	0.25	20	2.2×10^5

FIGURE 5-3 ORBITAL DESCENT
ALTITUDE PROFILE

FIGURE 5-4 CONSTANT BANDWIDTH EXAMPLE

FIGURE 5-5 ORBITAL DESCENT AVERAGE ERROR

FIGURE 5-6 ORBITAL DESCENT RMS ERROR

FIGURE 5-7 ORBITAL DESCENT RMS ERROR WITH NOISE

5-10

FIGURE 5-8 VERTICAL DESCENT ALTITUDE PROFILE
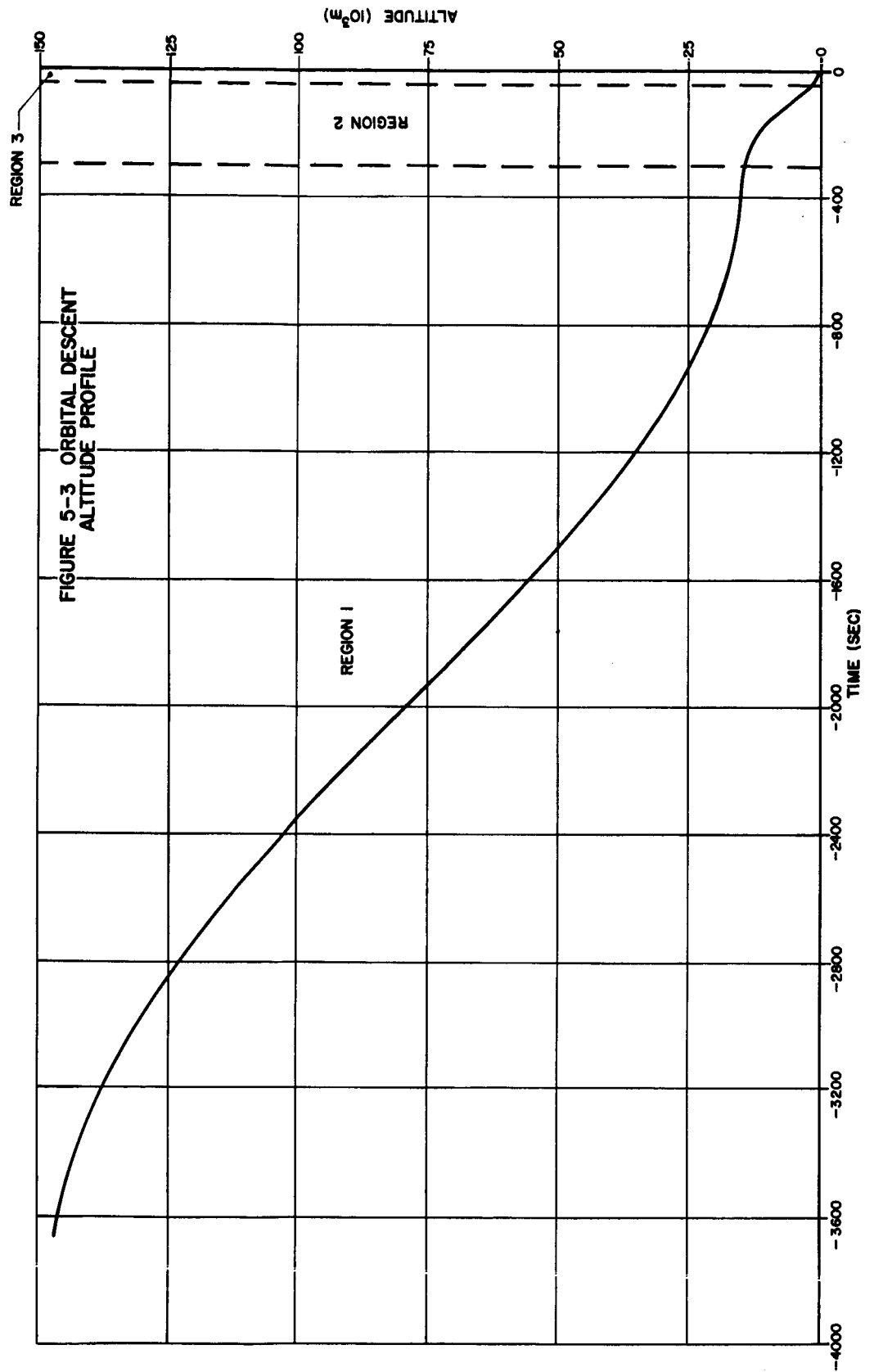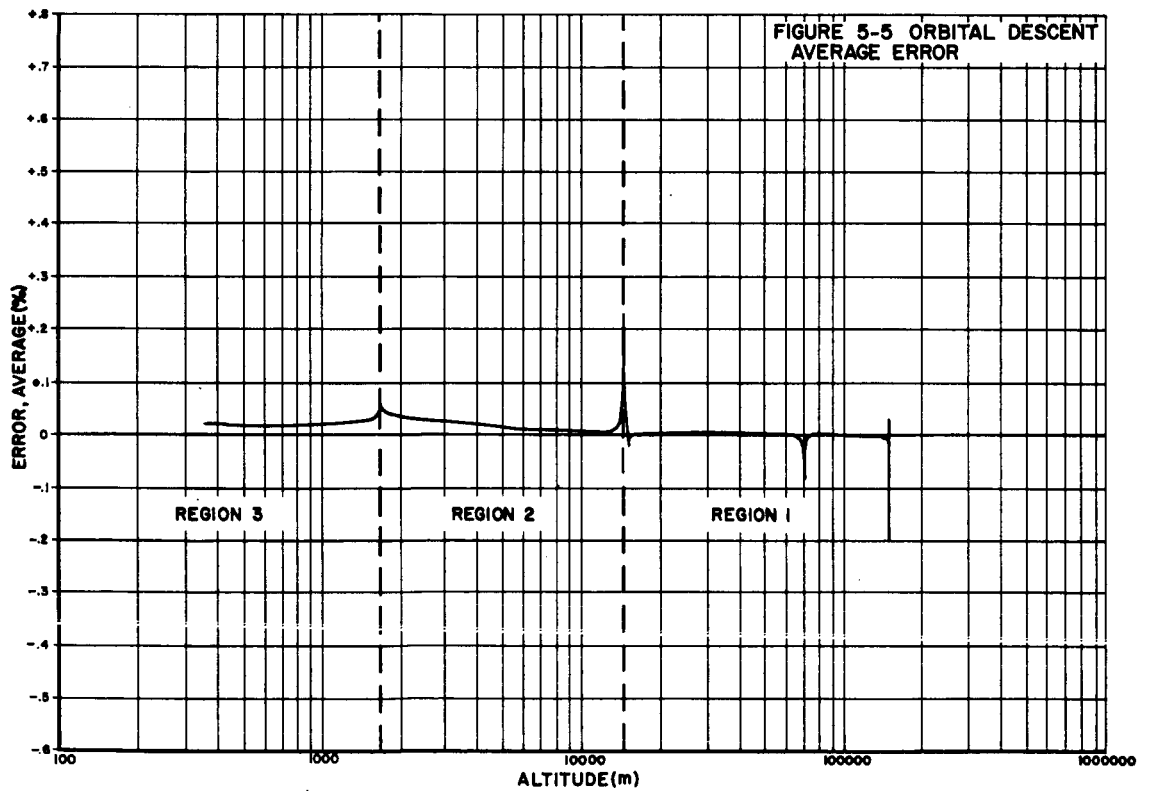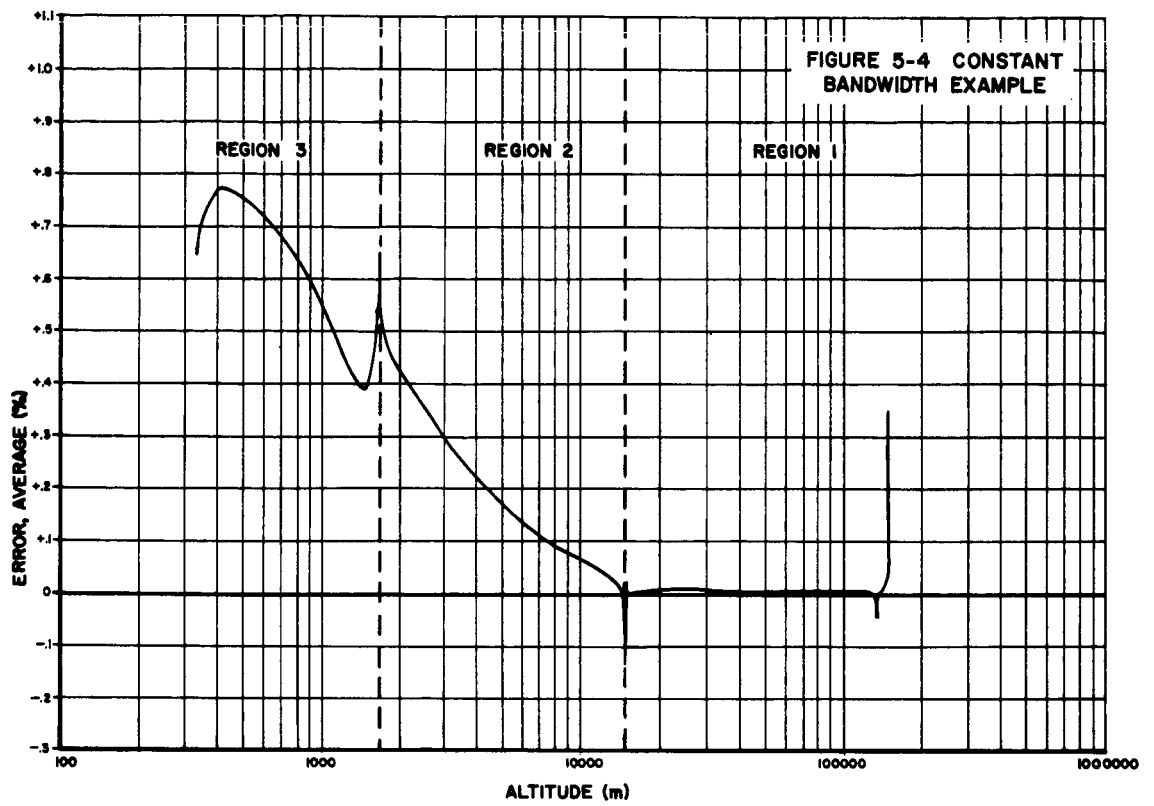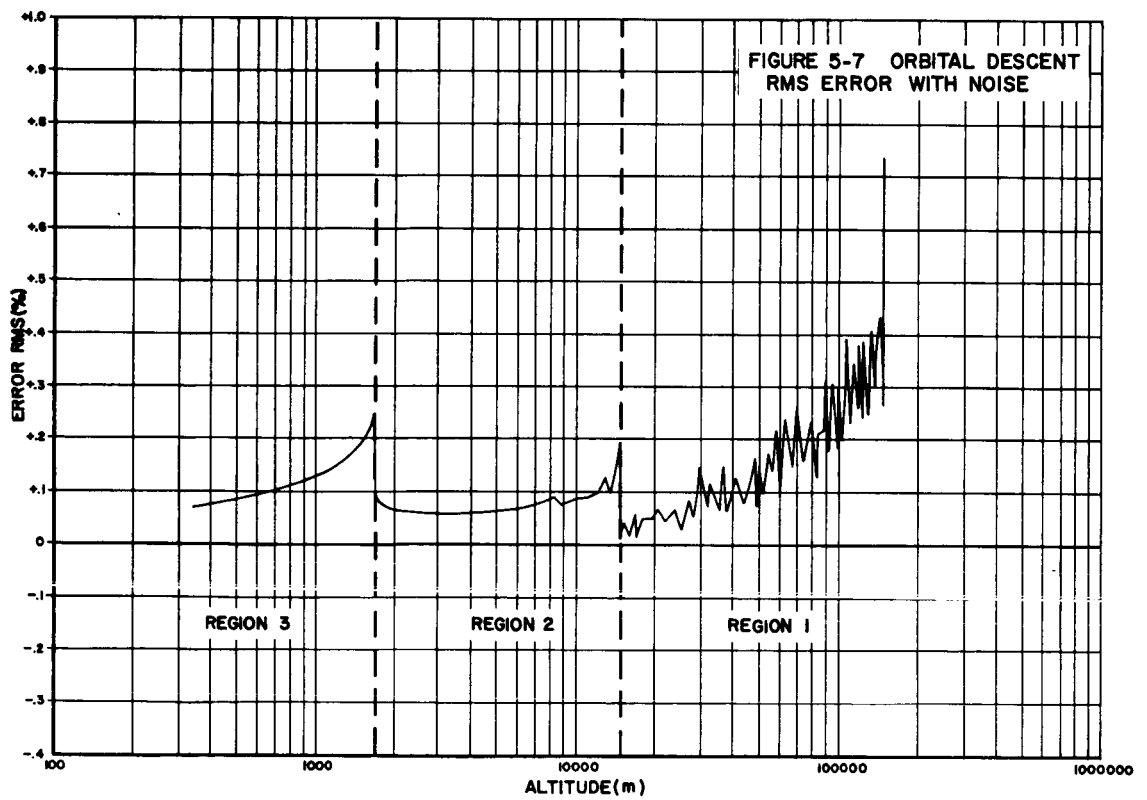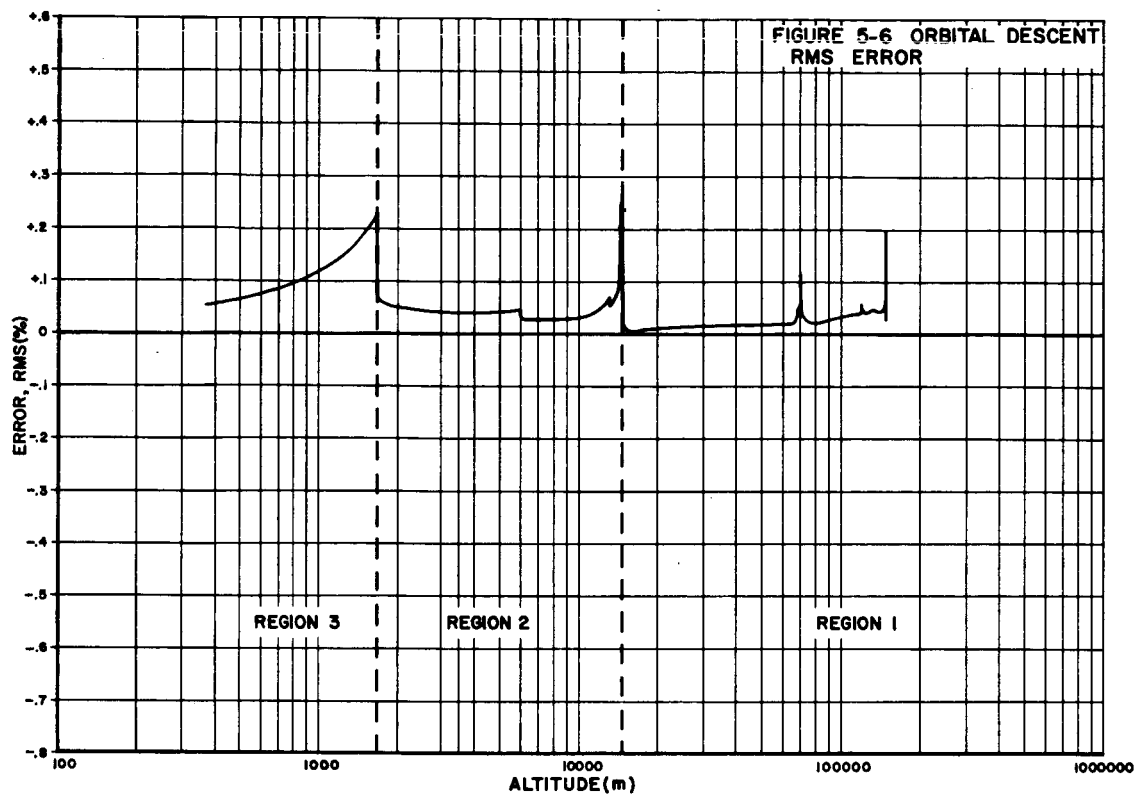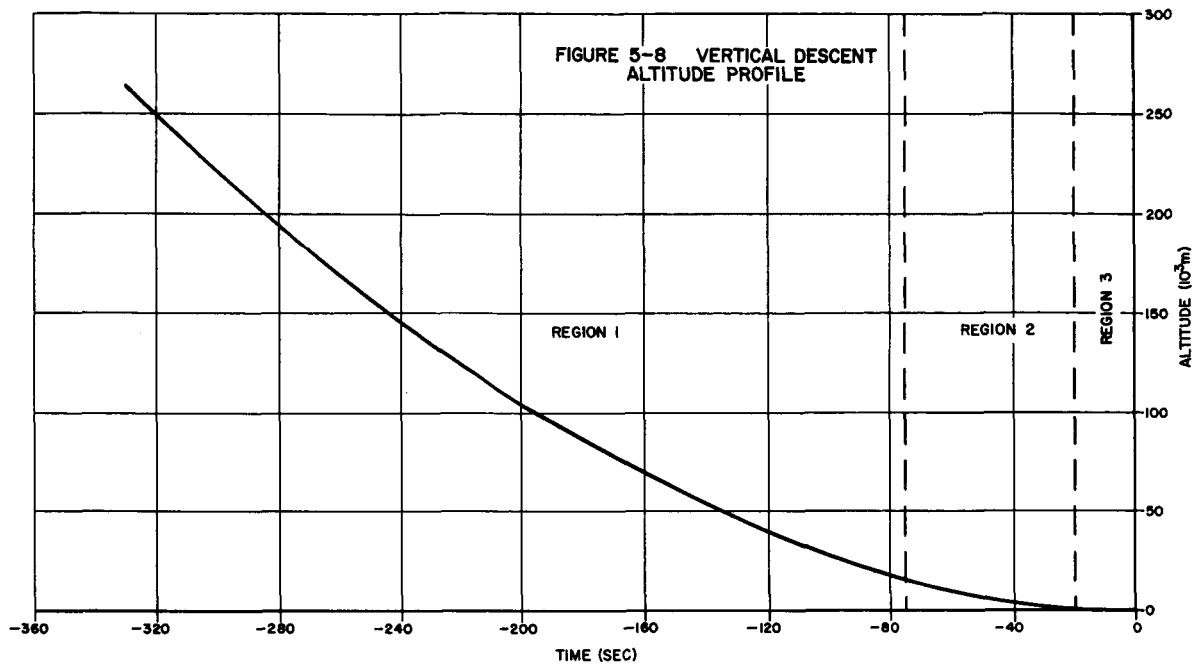
5.2.3. . . Test Case Profile

The test-case profile parameters are shown in Table 5-3, and the altitude profile used is presented in Figure 5-12. The descent was accomplished by applying five periods of constant deceleration as illustrated in Figure 5-12. In the intervals where the deceleration was not 9.14 m/sec^2, the spacecraft is in free flight. Velocity steps were incorporated at the origin of each region to fully stress the loop. Since this profile had the largest dynamic range, four regions were used instead of three in the investigation.

Table 5-3. Test-Case Altitude Tracking Loop Parameters

Region	Altitude (m)		Parameter Values				
	Maximum	Minimum	B_N(cps)	T_1(sec)	T_2(sec)	T_3(sec)	K_v
1	264,600	17,360	0.3	7.900	2.500	80	2.2×10^5
2	17,360	1,527	1.0	1.320	0.750	80	2.2×10^5
3	1,527	187	3.0	0.590	0.250	20	2.2×10^5
4	186	15.3	10.0	0.106	0.075	10	2.2×10^5

FIGURE 5-9 VERTICAL DESCENT AVERAGE ERROR

FIGURE 5-10 VERTICAL DESCENT RMS ERROR

FIGURE 5-11 VERTICAL DESCENT ERROR WITH NOISE

$-\ddot{h}=9.14\ m/SEC^2$

REGION I

TIME

−420	−400	−380	−360	−340	−320	−300	−280	−260	−240	−220	

FIGURE 5-12 TEST CASE ALTITUDE PROFILE
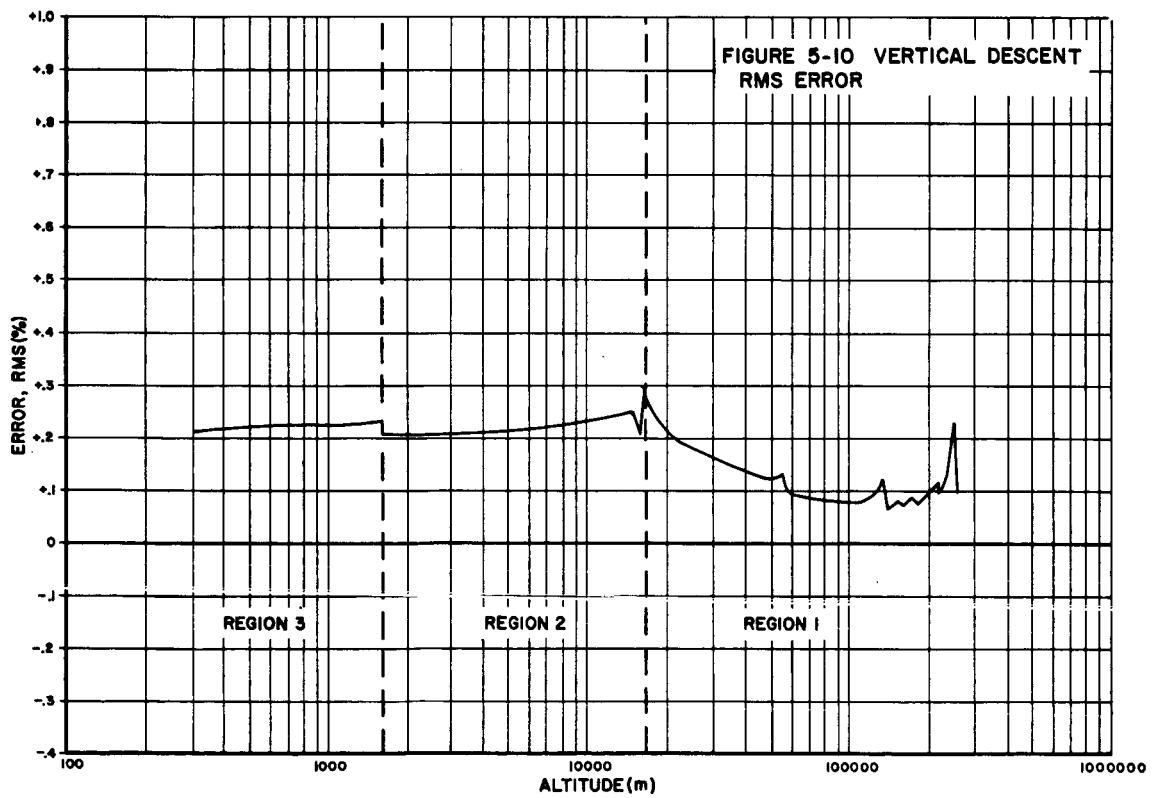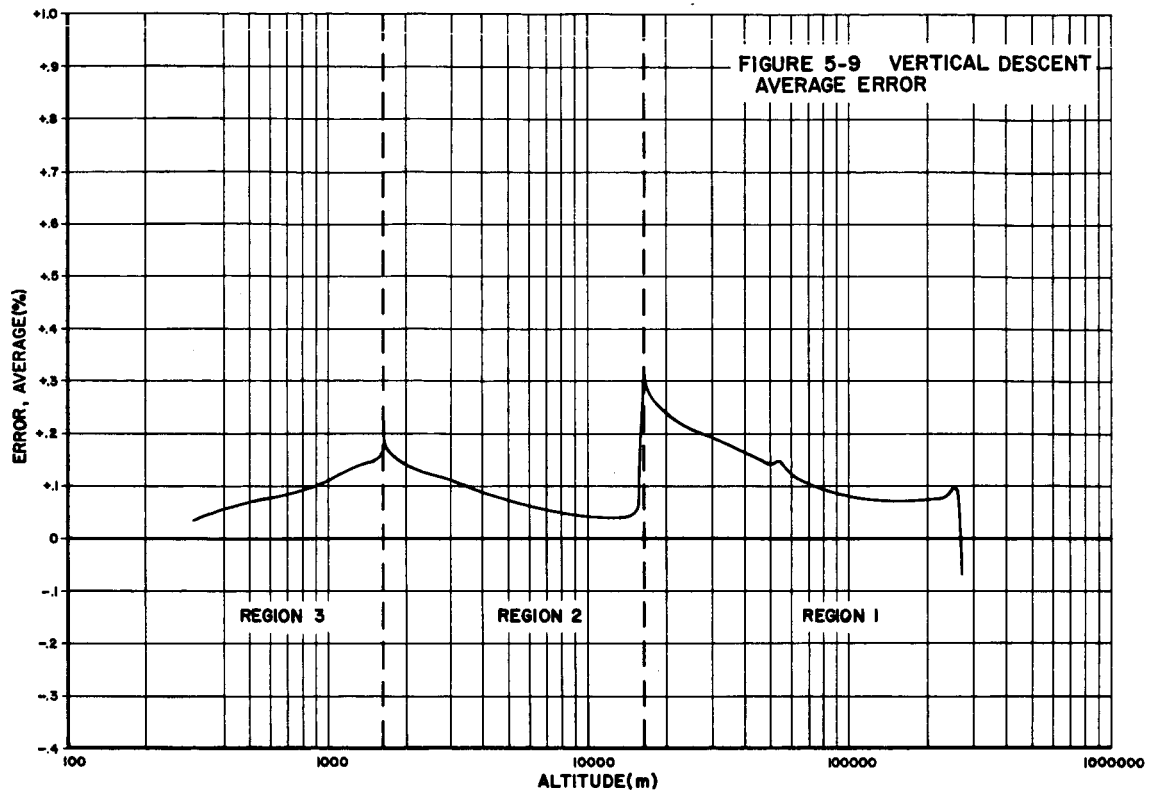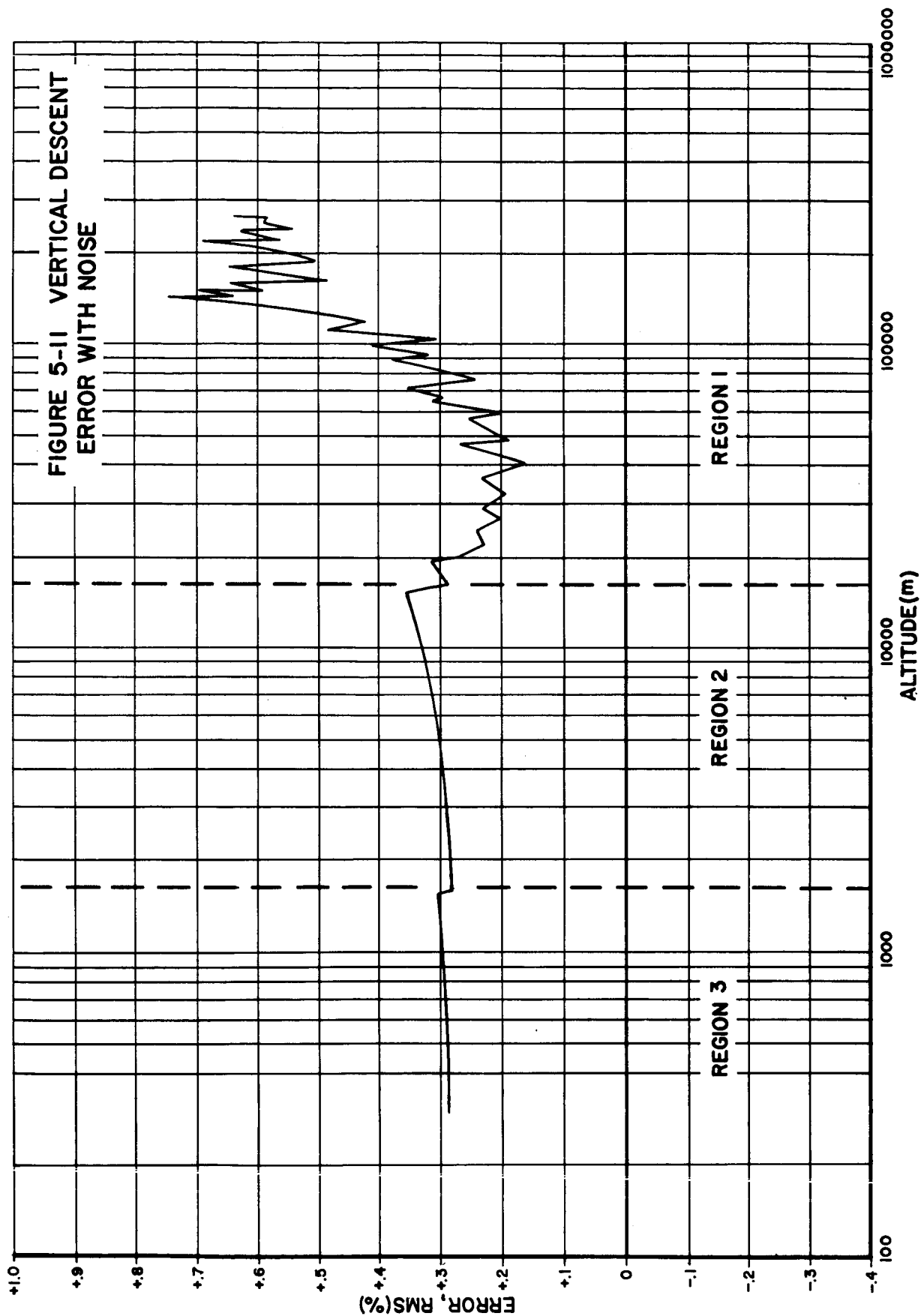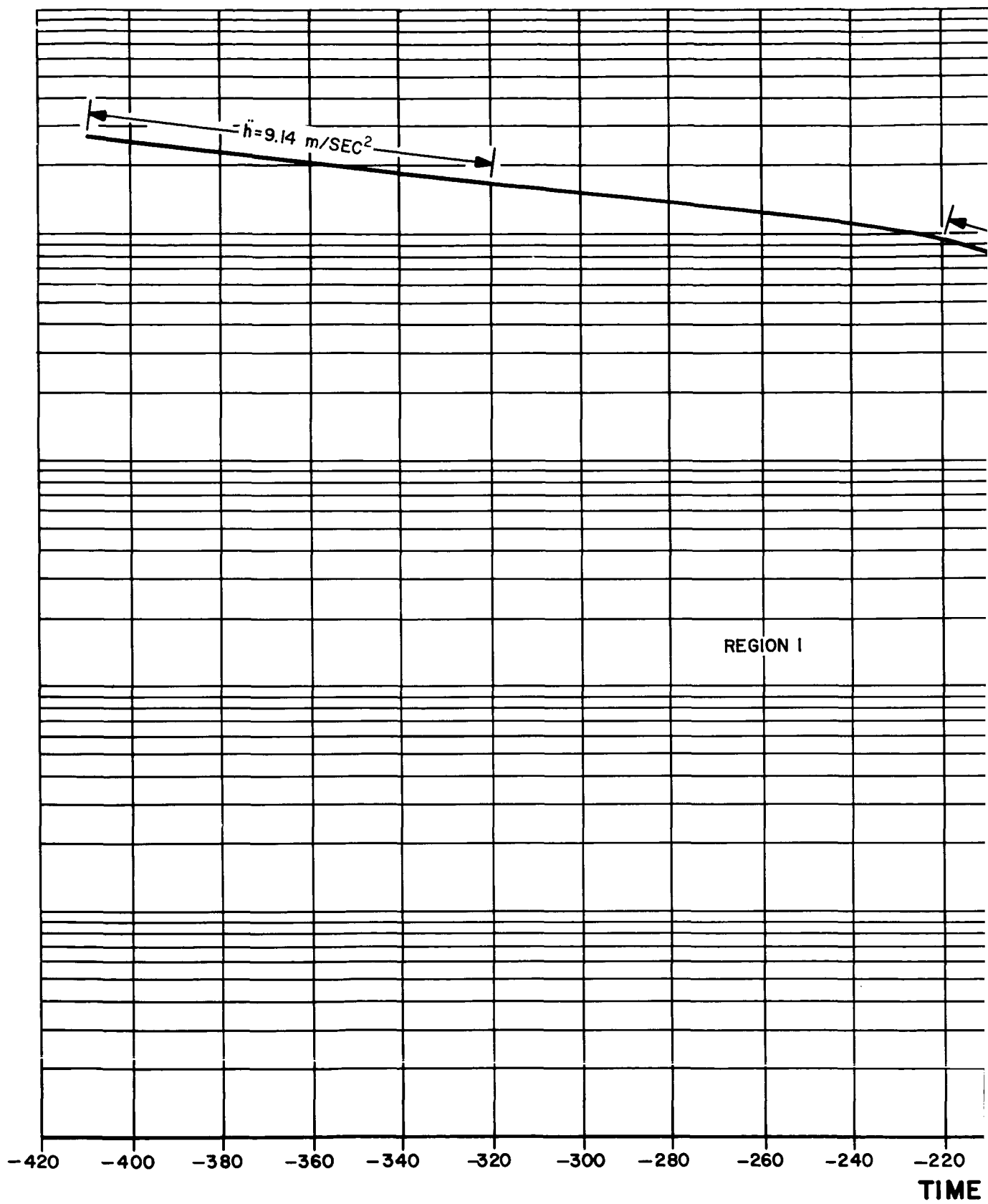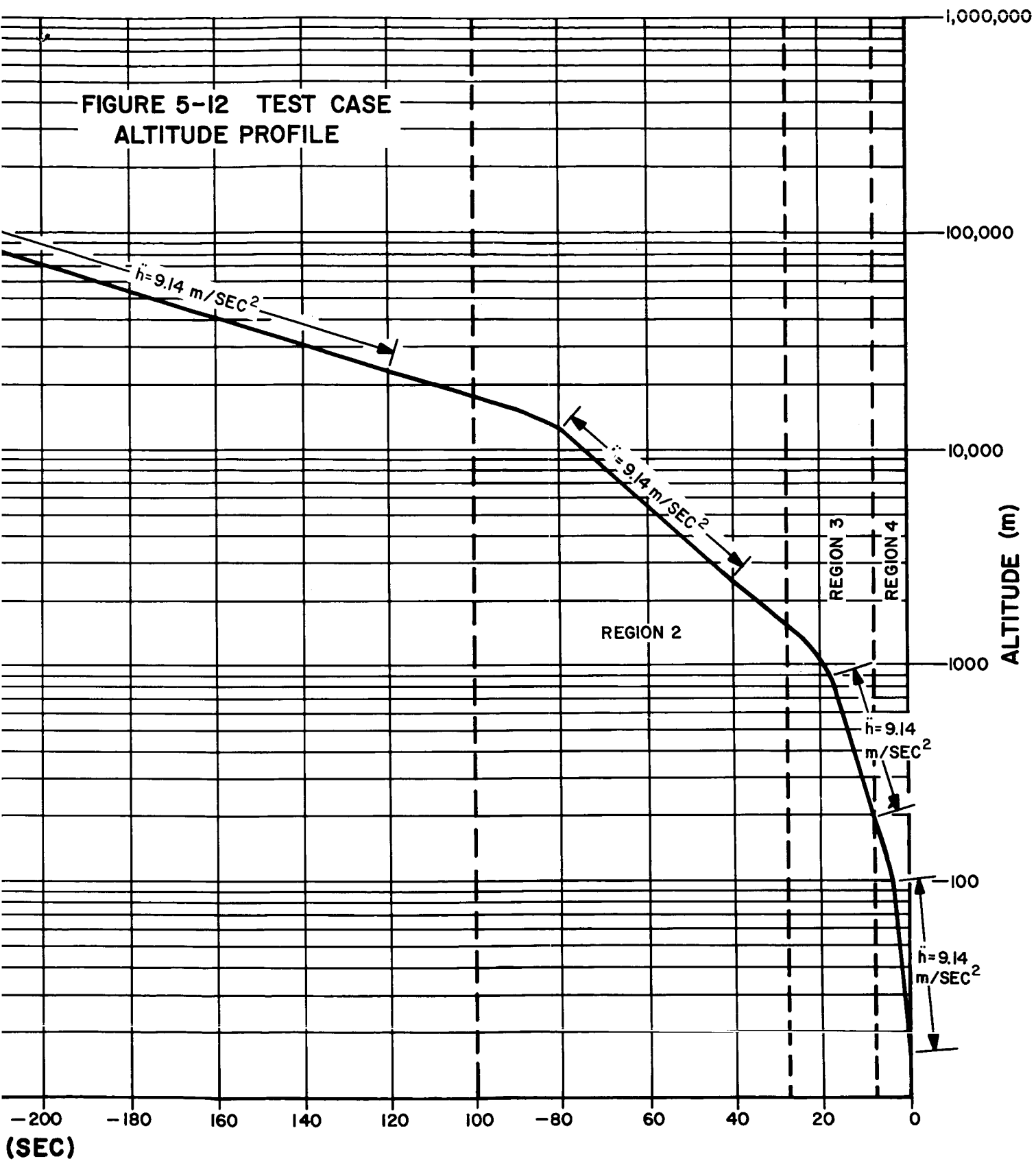
Figures 5-13 and 5-14 show the average and rms error, respectively, with no noise disturbance applied, and Figure 5-15 presents the rms error with a noise disturbance. Figure 5-16 shows the effect of removing the gain compensation. To show the effect of transients induced by the start of an acceleration period, data were taken using a 1-sec averaging process rather than the normal 10-sec smoothing. The effect of the reduction of the averaging period on the error is shown in Figure 5-17.

5.3 Discussion of Results

Because of the large dynamic range of altitude, both gain compensation and bandwidth switching will be necessary for satisfactory operation of the altitude tracking loop. The results shown in Figures 5-4 and 5-16 depict the effect of no bandwidth switching and no gain compensation, respectively. Gain compensation and bandwidth switching were used on all normal simulation runs.

The values for the performance parameters were nominally those chosen from the analysis in Interim Report No. 1. It should be noted that the value of T_3 was not maintained at 80 sec in the lower altitude regions. The change in T_3 was caused by a requirement for additional scaling in the analog computer which could not be accomplished readily. In the actual design, however, T_3 would conceivably be kept constant and only T_1 and T_2 would have to be changed to accommodate the bandwidth switching.

Certain trends can be observed from the error curves. Overall, the error decreased as the altitude was decreased and tended to show an (altitude)$^{1/2}$ dependence in the noise disturbance cases. The errors due to vehicle dynamics are well below the 0.5-percent specification. With the noise disturbance, this specification is exceeded at the higher altitudes with the specified smoothing times. As discussed in Interim Report No. 1, several alternatives are available to reduce the error. Included among these are (1) an increase in smoothing time to 17 seconds; (2) orientation of the vehicle to direct the altimeter beam nearer to vertical so as not to incur the -10-db scattering coefficient assumed in the power budget; (3) decrease in receiver noise figure by use of a low-noise parametric amplifier; (4) larger antenna aperture; and/or (5) an increase in transmitter output power. As indicated in Interim Report No. 1, an increase in the smoothing

FIGURE 5-13 TEST CASE AVERAGE ERROR

FIGURE 5-14 TEST CASE RMS ERROR

FIGURE 5-15 TEST CASE RMS ERROR WITH NOISE

FIGURE 5-16 TEST CASE WITH OPEN GAIN CONTROL LOOP

FIGURE 5-17 TEST CASE AVERAGE ERROR WITH ONE SECOND AVERAGING
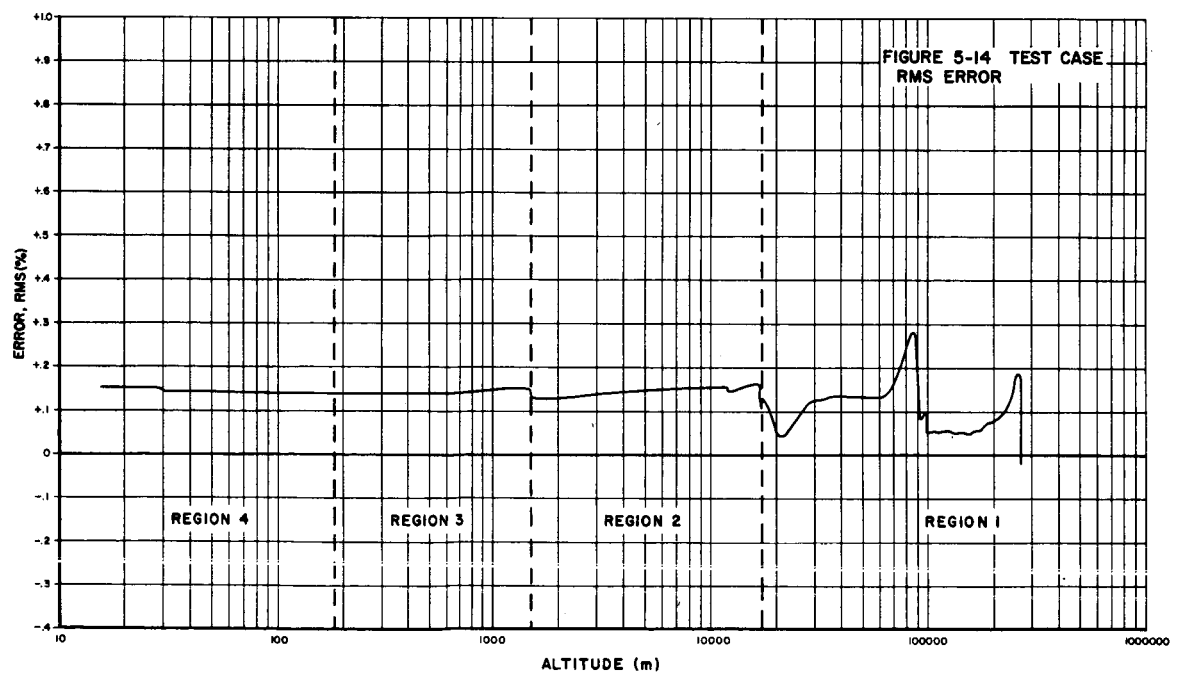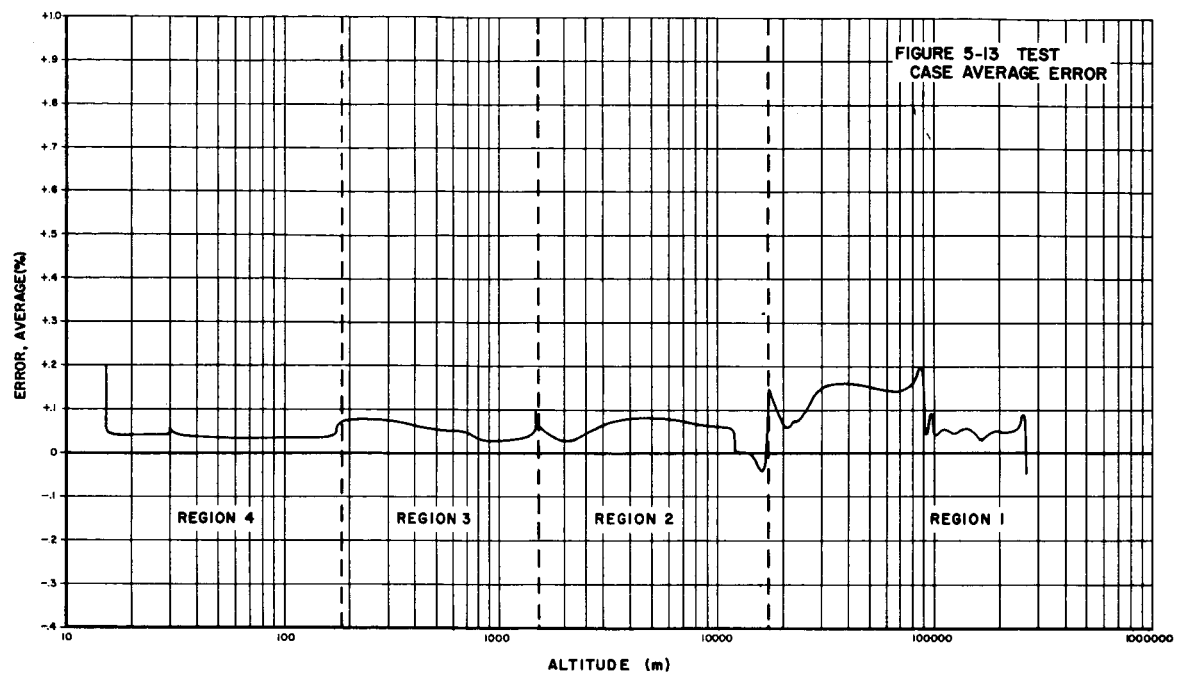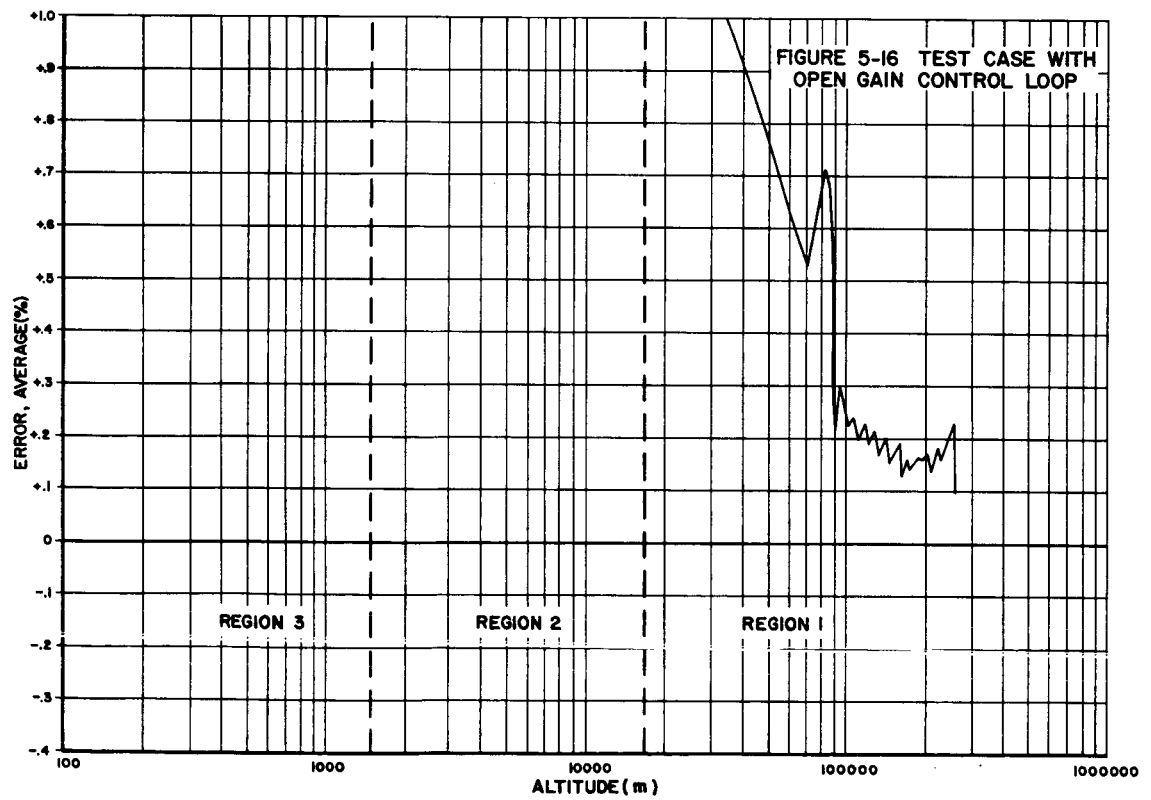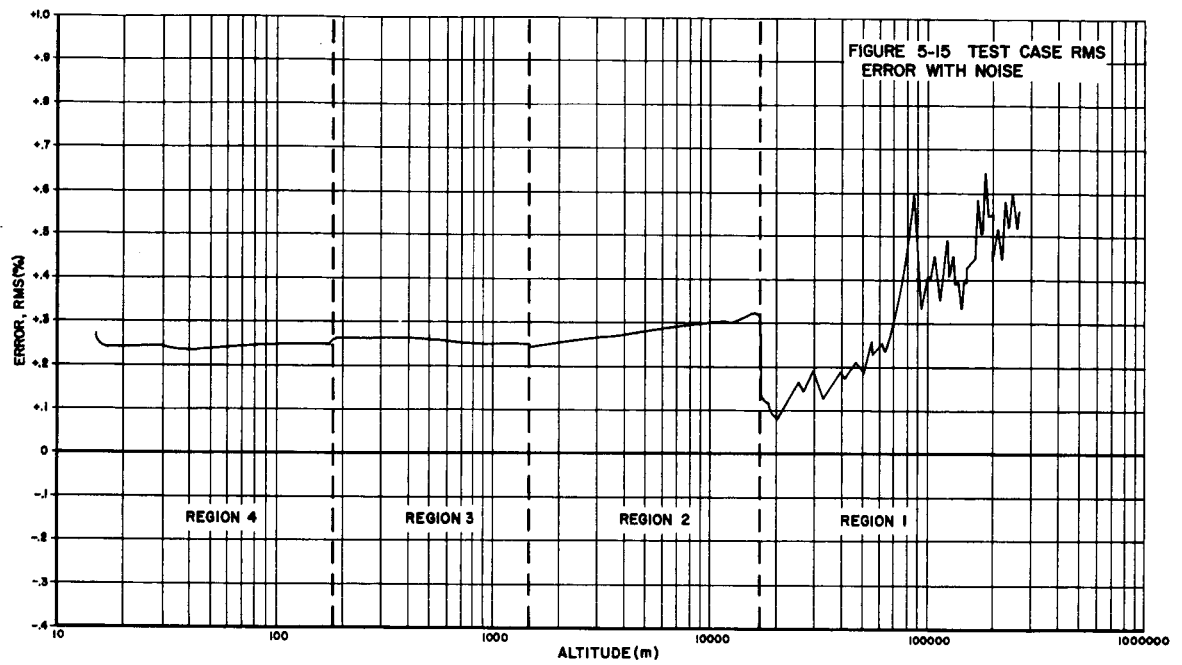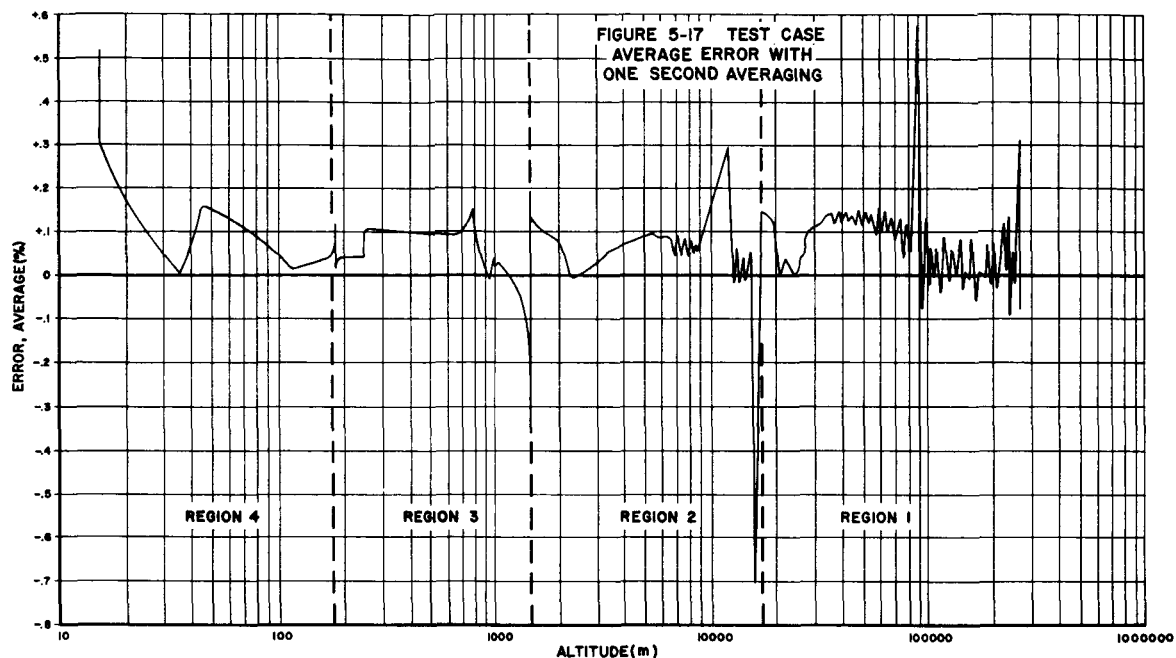
interval at high altitudes is preferred and causes no increase in equipment complexity or weight. The additional smoothing would be accomplished in the data processor. An uncooled, X-band parametric amplifier can reduce the receiver noise figure by at least 5 db for a weight penalty of 2 pounds. Correspondingly, improvements in performance of gallium antimonide tunnel diodes are anticipated within the next year to permit achievement of 4-db noise figures at X-band. This reduction in noise figure assumes, of course, that the noise temperature in the antenna's field of view does not exceed $400^{\circ}K$. The effects of a larger antenna aperture, i.e., greater than 60 cm, are increases in weight and storage volume.

Transient errors have not received attention in previous studies and must be considered in the actual design of the altitude tracking loop. Aside from lock-on, the most likely origin of transients will be acceleration discontinuities. The simulation using the test-case profile disclosed the nature of the transient errors likely to be encountered. The magnitude of the transient errors can be observed from the results of a typical simulation run shown in Figure 5-17. This plot was obtained with a short

smoothing time, 1 sec, rather than the normal recording smoothing of
10 sec, to disclose the fine structure of the error rather than the average.
An actual design will require a compromise between transient and steady-
state performance.

5.4 Conclusions

A simulation of the altitude tracking loop over the full dynamic
range of three altitude profiles was achieved using a hybrid analog-to-digital
computer. The need for both gain compensation and bandwidth switching was
demonstrated and fulfilled in the simulation. The tracking loop parameters
derived from the analysis of Interim Report No. 1 were used and proved the
basic validity of the analytical model. It was also shown that errors due to
acceleration and compensation discontinuities will have to be considered in
an actual design.

Appendix A.   COMPUTER BLOCK DIAGRAMS

The following figures present the actual working diagrams used to produce the hybrid simulation of the altitude tracking loop.   Figure A-1 presents the digital-computer flow chart.   Figures A-2 and A-3 present the analog-computer block diagrams with the former showing the compensation network of which four were required to accommodate the maximum of four regions used throughout the altitude profile.   Figure A-3 presents the implementation used for processing the data in the analog computer prior to plotting

```
                                                          ┌──────────────┐
                                                          │  045/06      │
              ┌─────────┐                                 │ PICKUP LDA   │
              │  TYPE   │                                 │        o-1   │
              │  "C"    │                                 │ AND STORE IN 015/16 │
              └────┬────┘                                 └──────┬───────┘
                   │ 337/02                                      │ 052/06
         ┌─────────▼─────────┐                          ┌────────▼────────┐
         │ MOVE DAC NUMBERS  │                          │   DETERMINE     │
         │   TO LINE 00      │                          │ REGION NUMBER   │
         └─────────┬─────────┘                          └────────┬────────┘
                                                                 │
  ┌────────┐                                            ┌────────▼────────┐       ┌──────────────────┐
  │ END    │                                            │ MOVE CONSTANTS  │       │ OUTPUT PULSE FOR │
  │ OF     ├────────────────────────►                   │  FOR REGION     │       │ SCALE CHANGE.(TO)│
  │ RUN    │                                            │  INTO LINE 16   │       │ REMAIN ON IN "ic"│
  └────────┘                                            └────────┬────────┘       └────────┬─────────┘
                                                                 │ 172/06                  │ 135/07
                   │ 000/06                             ┌────────▼────────┐       ┌────────▼─────────┐
         ┌─────────▼─────────┐                          │ SET CONSTANTS   │       │ PICKUP DAC       │
         │ RESET LOGIC UNIT  │                          │ INTO LINES 04   │       │          S.C. FOR│
         │ SET R(-) AND S(-) │                          │ AND 03 TO       │       │ SCALE CHANGE AND │
         └─────────┬─────────┘                          │ USE IN COMPUTER │       │ STORE FOR LATER  │
                                                        └────────┬────────┘       │ USE              │
                   │ 010/06                             ┌────────▼────────┐       └──────────────────┘
         ┌─────────▼─────────┐                          │ SET Σ Δt = 0    │
         │ SAMPLE ANALOG     │                          │ OUTPUT K_max    │
         │ INPUT "ic"+ 10^V  │                          │         ─────   │
         └─────────┬─────────┘                          │         H_max   │
                                                        └────────┬────────┘
                   │ 021/06                                      │ 256/06
              ◇────▼────◇                               ┌────────▼────────┐       ┌──────────────────┐
              │  TEST   ├──────────┐                    │ PICKUP LDA      │       │ SET ITERATION    │
              │  "ic"   │          │                    │          o-1    │       │ FLAG             │
              ◇────┬────◇          │                    │ AND INCREMENT   │       └──────────────────┘
                   │ NOT           │                    └────────┬────────┘              │ 342/06
                   │ "ic"          │
                   │          ◇────▼────◇
                   │          │  TEST   ├──────────►
                   │          │  S(+)   │
                   │          ◇────┬────◇
                   │               │ (+)
         ┌─────────▼─────────┐     │
         │  INPUT "H" + 10^V  │◄────┘                   ┌────────▼────────┐       ┌──────────────────┐
         └─────────┬─────────┘                          │ LOAD h ,h ,h    │262/06 │ ANALOG TO HOLD.  │
                                                        │      o  1  2     │       │ DELAY IN HOLD.   │
                   │ 040/06                             │ AND STORE.      │       └────────┬─────────┘
              ◇────▼────◇                               │ SET h  = h      │
              │  TEST   │  "H"                          │      o    e     │
              │  "H"    ├──────────►                    └────────┬────────┘
              ◇────┬────◇                               ┌────────▼────────┐       ┌──────────────────┐
                   │ NOT                                │ COMPUTE INITIAL │       │ RELEASE SCALE    │
                   │ "H"    042/06                      │ f  AND f , STORE│       │ CHANGE PULSE     │
              ◇────▼────◇  OFF                          │  1      2       │       └────────┬─────────┘
              │  TEST   ├──────────►                    └────────┬────────┘                │ 240/07
              │ BREAK POINT │                                    │ 357/06         ┌────────▼─────────┐
              ◇────┬────◇                               ┌────────▼────────┐       │ SET R(-).        │
                   │ ON                                 │ PICKUP LDA  AND │       │ DELAY IN "ic"    │
                   │ 013/02                             │           o     │       └──────────────────┘
              ┌────▼────┐                               │ INCREMENT TO LDA│
              │  READ   │                               │             e+3 │
              │ ROUTINE │                               └────────┬────────┘
              └─────────┘                                        │ 364/06
                                                            ◇────▼────◇
                                                            │  TEST   │  (+)
                                                            │  S(+)   ├──────────►
                                                            ◇────┬────◇
                                                                 │ (-)
                                                                 │ 366/06
                                                        ┌────────▼────────┐
                                                        │ SET S(+).       │
                                                        │ SET TRANSFER    │
                                                        │ OUT OF LINE 16  │
                                                        └────────┬────────┘
                                                        ┌────────▼────────┐
                                                        │ CLEAR LOCATION  │
                                                        │ OF DAC          │
                                                        │        S.C.     │
                                                        └─────────────────┘
```

Partial boxes at right edge:

- ANALOG ... DELAY I...
- RESET LO... ANALOG ...
- END ... RU... (decision) — NO
- OUTPUT TO...
- E... O... RU... (decision)
- SAM... ANA... DAT...
- CON... DIG... DA...
- INCRE... ITERA... FLA...

FIGURE A-1. DIGITAL COMPUTER FLOW CHART.

Column 1 (left partial):

026/0?

TO HOL HOLD.

IC UNIT. TO I.C.

125/07

OF N? YES

RESET A40.

000/06

LE OG

VERT TAL TA

254/04

MENT TION

ITERATE ERROR

Center-left column:

015/16 — PICKUP NEXT h_{n+2} AND TRANSFER BACK TO LINE 03

020/03 — END OF REGION FLAG? YES / NO

021/03 — UPDATE h_n, h_{n+1}, h_{n+2}. UPDATE h_{n+2} PICKUP.

PICKUP h_n AND SET $h_n = h_t$

PICKUP h_{n+1} AND SET $\Sigma \Delta t = 0$

COMPUTE f_1 AND f_2

201/04 — CLEAR SHIFT REGISTER. INPUT $2^n\, Ka/100$ ($\Delta\, 1/h_r$)

SHIFT $2^n\, Ka/100$ ($\Delta\, 1/h_r$) RIGHT n BITS

ADD $Ka/100\,(1/h_r)h-1$ ⟶ $Ka/100(1/h_r)_n$

STORE AND OUTPUT $Ka/100\,(1/h_r)_n$

243/04 — TEST FLAG (−) / (+)

246/04 — MULTI $100/Ka \times Ka/100\; 1/h_r$ ⟶ $1/h_r$. STORE.

Center column:

COMPUTE (circle)

002/03 — COMPUTE $\Sigma \Delta t - (T - \epsilon)$

TEST $\Sigma \Delta t > T - \epsilon$ YES / NO

015/04 — UPDATE $\Sigma \Delta t$. COMPUTE $h_n + f_1 \Sigma \Delta t$.

071/04 — COMPUTE $(T - \Sigma \Delta t)$, $\Sigma \Delta t\,(T - \Sigma \Delta t)$, AND $f_2 \Sigma \Delta t (T - \Sigma \Delta t)$

167/04 — COMPUTE $h_t = h_n + f_1 \Sigma \Delta t + f_2 \Sigma \Delta t (T - \Sigma \Delta t)$

COMPUTE $-E(t) = \pi (h_s/h_r - 1)$ AND STORE

PREPARE h_t FOR OUTPUT

COMPUTE $(h_t - h_r)$ AND PREPARE FOR OUTPUT

PREPARE $-E(t)$ FOR OUTPUT

TEST $R(\pm)$ CONTINUE / (−)

004/07 — SET $R(\pm)$.

Right column:

337/03 — TEST E.O.C.

TEST BREAK POINT OFF CONTINUE / ON

346/07 — ANALOG TO HOLD MODE

RESET LOGIC UNIT

CLEAR SHIFT REGISTERED INPUT "H" + 10^v

TEST "H" NOT "H" CONTINUE / "H"

374/07 — RESET LOGIC UNIT

376/07 — SAMPLE ANALOG DATA AND CLEAR SHIFT REGISTER.

INPUT "ic" + 10^v

210/07 — TEST "ic" "ic" / NOT "ic"

INPUT "o" + 10^v

230/07 — TEST "o" NOT "o" / "o"

334/07 — START TIMER

002/03 — COMPUTE (circle)

000/06 — END OF RUN

$-\left(\begin{matrix}15.000\\1.500\\0.150\\0.015\end{matrix}\right)\left(\dfrac{h_{max}}{h_t}\right)e_i$

DAC T43 $-300\,E(t)$ 24 1 ⓪25 $K_d/2$ 1 25 1 $-150\,e_i$ M03 X Y

N.C. A 2/

NOISE GEN T10 1 F106 U.

D. ⑭141 $K/10$ 10 F06 X M06 Y

$K_m K_h K_t (h_t/h_m)$

U. FS-13 D. ⓹50 0.1 $+100^v$

A R K03 ⑯116 $.08$ $+100^v$

N.O.

N.C. A

A R K04 ⑬139 0.18 $+100^v$

N.O.

DAC T56 $K_m K_t/h_m$ M07 X Y

$+100^v$ ⓩ24 1 F10T 1 $h_{max}/6.67\times10^6$

DAC T46 $+K_h h_t$ 1 33 $\dfrac{h_{max}/h_t}{6.67\times10^2 K_n}$ X M02 Y +

U. $+100^v$ FS-12 -100^v D. ⓶202 0.0 1 40 G 1 A R K05 ⑭140 0.28 $+100^v$

DAC T53 SCALE CHANGE PULSE ④40 0.2

N.C. A N.O.

4/

4/

MODE CONTROLS

DAC T54 "ic" PULSE A R K00

$+5.6^v$ 1 F100

DAC T55 "H" PULSE R A K01

N.O. N.C. P03 I I "ic" P00 T47 ADC

N.O. N.C. P04 H H "H" P01 T48 ADC

C "O" P02 T49 ADC

IN OUT

4

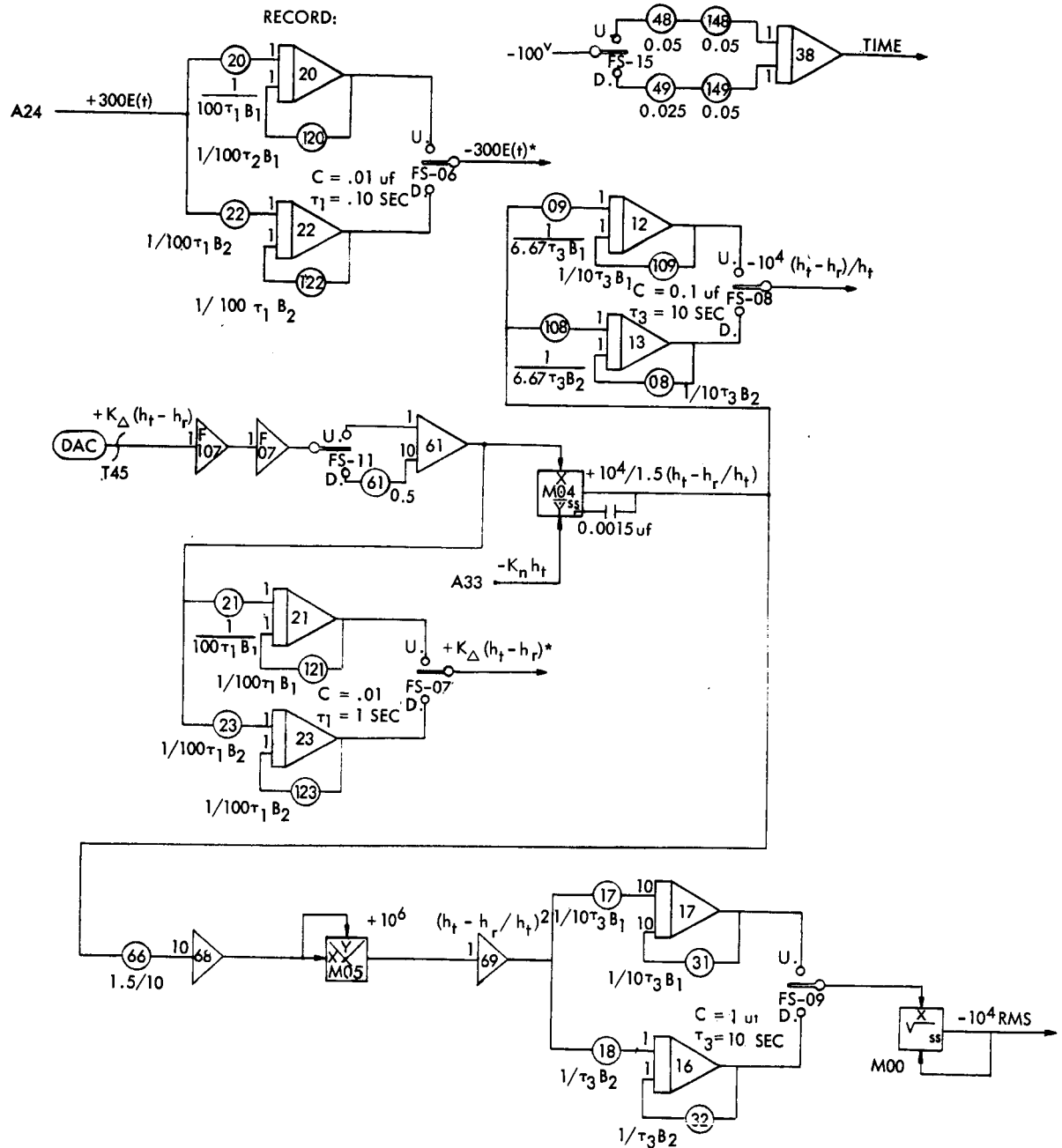FIGURE A-2. ANALOG COMPUTER BLOCK DIAGRAM

A-3

FIGURE A-3. ANALOG OUTPUT FOR RECORDING DATA.

Appendix B.   NOISE IN SIMULATION

This section derives the expression relating the recorded value of altitude error to the noise spectral density. A noise spectral density equal to one-quarter of that to be expected at any given altitude was employed in the simulation study to make the scaling problems tractable.

The noise used in the simulation of the altitude tracking loop had zero mean and was assumed to have at least linear independence with respect to the signal. Because of the linear independence of the signal and noise, and the fact that the noise had zero mean, the second moment of the sum of the signal voltage, s, and the noise voltage, n, which is the total power, is given by

$$\overline{(s + n)^2} = \overline{s^2} + \overline{n^2} \tag{B-1}$$

Therefore, the noise is given by

$$\overline{n^2} = \overline{(s + n)^2} - \overline{s^2} \tag{B-2}$$

If the noise power is now scaled by a constant a , the new total power

is found from

$$\overline{(s + n)^2_{actual}} = \overline{a(s + n)^2} - (a - 1)\overline{s^2} \tag{B-3}$$

In the case of the simulation, to find the rms error due to the actual noise power spectral density, i.e.,

$$(s + n)^2_{actual}$$

a value of four must be used for a. Thus, the rms error for the actual noise power can be found from

$$\sqrt{\overline{(s + n)^2}_{actual}} = \sqrt{\overline{4(s + n)^2}} - \overline{3s^2} \qquad (B-4)$$

where $\overline{(s + n)^2}$ is the square of the recorded rms signal plus noise error and $\overline{s^2}$ is the recorded rms signal error. Evaluating the test case at an altitude of 220 km, which yielded values for $\sqrt{\overline{(s + n)^2}}$ of 0.55 percent rms altitude error and for $\sqrt{\overline{s^2}}$ of 0.10 percent rms altitude error, the total error due to the actual noise is found from Equation (B-4) to be 1.07 percent rms error. The altitude value of 220 km was used since this was the maximum altitude considered in Interim Report No. 1 and an analytical comparison could readily be obtained. The rms error of 1.07 percent because of noise introduced in the simulation compares quite favorably with the previously estimated 0.9 percent rms noise error.